Anna Frick

Structural Studies of Aquaporins in Human Kidney and Plant

Faculty of Science

ISBN 978-91-628-8661-5
Printed by Ineko

2013

Structural Studies of Aquaporins in Human Kidney and Plant

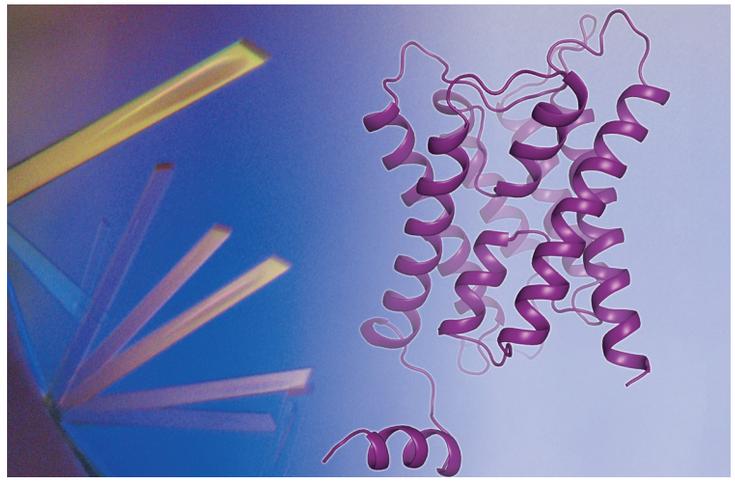

Anna Frick

Ph.D. thesis
Department of Chemistry and Molecular Biology
University of Gothenburg

UNIVERSITY OF GOTHENBURG

THESIS FOR THE DEGREE OF DOCTOR OF PHILOSOPHY IN NATURAL SCIENCE

Structural studies of aquaporins in human kidney and plant

ANNA FRICK

GÖTEBORGS UNIVERSITET

University of Gothenburg

Department of Chemistry and Molecular Biology

Göteborg, Sweden, 2013

Structural studies of aquaporins in human kidney and plant

Anna Frick

Cover: Crystals and structure of human aquaporin 2.

ISBN 978-91-628-8661-5
Available online at http://hdl.handle.net/2077/32281

University of Gothenburg
Department of Chemistry and Molecular Biology
Lundbergslaboratoriet
SE-405 30 Gothenburg
Sweden
Telephone: +46 (0)31-786 0000

Printed by Ineko AB
Göteborg, Sweden 2013

Till farmor och mormor

Abstract

Membrane proteins are key players in our biology and are links between the inside and the outside of the cell, allowing for signal transduction and transport of molecules. Aquaporins are membrane protein channels that allow water to pass in and out of the cell. Since all life depend on water, their function is vital for any type of organism. Although aquaporins are very similar, they have small but important differences in their structure and function. Understanding these subtle dissimilarities helps us understand the fundamentals of our biology and is also essential if aquaporins are to be used as drug targets.

This thesis has investigated the structure and function of two aquaporins from different species; human and spinach. The spinach aquaporin SoPIP2;1 has become the structural model for gated plant aquaporins. In this thesis, structural and functional data is presented that gives further insights into the gating mechanism controlled by the physiological signals phosphorylation, pH and divalent cations. In addition, the mechanism behind the activation of SoPIP2;1 by mercury, commonly regarded as an aquaporin blocker, has been studied.

Human Aquaporin 2 is crucial for the kidneys ability to concentrate primary urine, and its malfunction leads to nephrogenic diabetes insipidus. An X-ray crystallographic structure to 2.95Å is presented, which show that AQP2 is markedly different also from its most closely related homologues. These differences are mainly focused on loop D and the C-terminus and can be related to binding of Cd^{2+} in the structure. We present data that Cd^{2+} could correspond to Ca^{2+} in vivo, and discuss the role of the C-terminal helix as a protein interaction partner. In addition, mutations leading to nephrogenic diabetes insipidus are studied in the structural context.

List of Publications

Paper I Nyblom M, **Frick A**, Wang Y, Ekvall M, Hallgren K, Hedfalk K, Neutze R, Tajkhorshid E, Törnroth-Horsefield S. "Structural and functional analysis of SoPIP2;1 mutants add insights into plant aquaporin gating". *J.Mol. Biol.* 387(3):653-668 (2009)

Paper II **Frick A**, Järvå M, Törnroth-Horsefield S. "Structural basis for pH gating of plant aquaporins." *FEBSLett.* 2013 Feb 26. doi:pii: S0014-5793(13)00184-1. 10.1016/j.febslet.2013.02.038. *Epub ahead of print*

Paper III **Frick A**, Järvå M, Ekvall M, Uzdavinys P, Nyblom M, Törnroth-Horsefield S. "Mercury activation of the plant aquaporin SoPIP2;1 - structural and functional characterization". *Submitted to Biochemical Journal*

Paper IV **Frick A**, Kosinska-Eriksson U, Öberg F, Hedfalk K, Neutze R, de Grip W, Deen P, Törnroth-Horsefield S. "X-ray structure of human AQP2 at 2.95 Å resolution". *Manuscript*

RELATED PUBLICATIONS

Paper V Gourdon P, **Alfredsson A**, Pedersen A, Malmerberg E, Nyblom M, Widell M, Berntsson R, Pinhassi J, Braiman M, Hansson Ö, Bonander N, Karlsson G, Neutze R. "Optimized in vitro and in vivo expression of proteorhodopsin: a seven-transmembrane proton pump". *Protein Expr Purif.* 58(1):103-13 (2008)

Contribution report

Paper I I produced, purified and crystallized the protein. I conducted some of the functional assays. I wrote a minor part of the manuscript and prepared figures.

Paper II I produced and crystallized the protein. I took part in analyzing the structure, writing the paper and preparing the figures.

Paper III I planned the project, produced, purified and crystallized the protein. I collected and processed the diffraction data. I solved, refined and analyzed the structure. I was involved in the functional assays. I took major part in writing the manuscript and prepared figures.

Paper IV I planned and performed most of the experimental work. I solved, refined and analyzed the structure. I prepared figures and took part in writing the manuscript.

Contents

Abbreviations

AQP	Aquaporin
AVPR2	Arginine vasopressin receptor 2
β-OG	n-octyl-β-D-glucopyranoside
cAMP	cyclic adenosine monophosphate
CMC	Critical Micelle Concentration
EM	Electron Diffraction
ER	Endoplasmatic Reticulum
ERAD	Endoplasmatic Reticulum associated degradation pathway
hAQP	human Aquaporin
IMAC	Immobilized Metal Affinity Chromatography
MIP	Major Intrinsic Protein
MD	Molecular dynamics simulations
NDI	Nephrogenic Diabetes Insipidus
NG	n-nonyl-β-D-glucopyranoside
NIP	Nodulin26-like intrinsic proteins
NPA	asparagines-proline-alanine signature motif of aquaporin
OD	Optical density
OGNPG	Octyl Glucose-Neopentyl Glycol
PDB	Protein Data Bank
PEGxxx	Poly Ethylene Glycol with an average length of xxx units
PIP	Plasma membrane Intrinsic Protein
PKA	Protein Kinase A
SIP	Small basic Intrinsic Protein
TIP	Tonoplast Intrinsic Protein
TM	TransMembrane helix
Å	Ångström

Species

At	*Arabidopsis thaliana* – mouse ear cress
Bv	*Beta vulgaris* – beet root
Bt	*Bos taurus* - cattle
Ec	*Escherichia coli* – *E.coli*
Mt	*Medicago truncatula* – Barrel clover
Oa	*Ovis aries* – sheep
Pp	*Pichia pastoris* - yeast
Zm	*Zea mays* - maize
So	*Spinacia oleracea* - spinach

1 Introduction

1.1 Membrane Proteins

All living organisms, no matter if it is a human or a bacterium, are made up of cells and cells are surrounded by a membrane. When this type of organization arose early in the history of life, it was a way of keeping the molecules needed for the necessary reactions together, as well as creating an optimal environment that was different from the outside. But, to rephrase a famous quote – no cell is an island. All cells need to register what is going on in the surroundings and adjust its actions accordingly. Some molecules must also be allowed to enter and exit the cells. For many fundamental reactions of our biology, such as energy generation, creating a gradient across a biological membrane is crucial. The molecules responsible for all these tasks are the membrane proteins. Incorporated into the lipid bilayer that constitutes the membrane, this diverse set of proteins performs tasks like signal transduction and transportation of molecules (Figure 1). Situated at this border, they hold a key position in many biological processes, and hence in disease states. Of our genes, about 25% code for a membrane protein [1] and they constitute more than 50% of current drug targets [2].

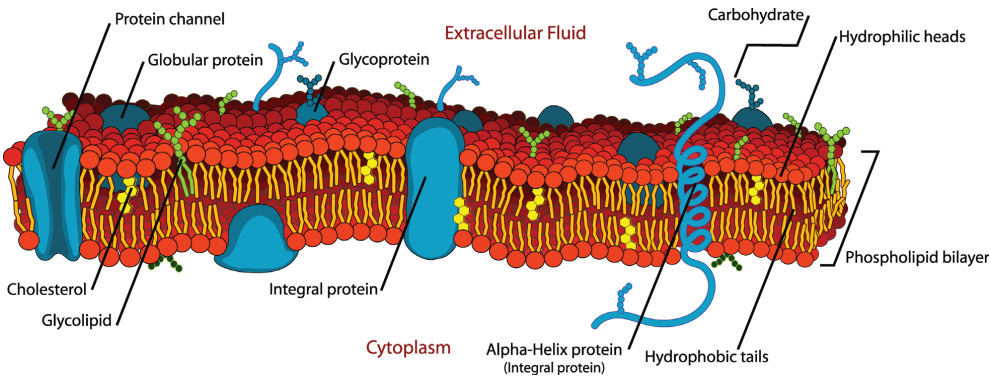

Figure 1. Schematic picture of the cell membrane. The lipids (red/orange) form the bilayer which contains a diverse set of proteins.

1.1.1 Membrane protein transport

Molecules that cannot pass membranes by diffusion through the bilayer must be helped by a transport protein of which different types exist. Some membrane proteins actively transport their substrate against a concentration gradient, requiring energy, while others allow passive passage for molecules that follows their concentration gradient. The molecules to be transported range from small molecules like protons, ions and water to larger molecules like sugars and amino acids and even macromolecules. The membrane protein transporters can also be divided into carriers and channels, where the former specifically interacts with its

substrate and cycle through several conformational states in the transport process. In contrast, channel proteins interact with their substrate more weakly and the transported molecule diffuses passively along their concentration gradient through a pore created by the protein. The aquaporins studied in this thesis belong to the channel protein class, which allow their substrate, in this case water, to pass the membrane in a very fast, passive diffusion process.

1.1.2 THE STUDY OF MEMBRANE PROTEINS

Structural studies of membrane proteins through X-ray crystallography are more difficult than their soluble counterparts in almost every aspect, from production to crystallization. While the first protein structure, myoglobin, was published in 1960 [3], it took until 1985 until the first membrane protein structure, a bacterial photosynthetic reaction center, was reported [4]. Still today, of the approximately 90 000 structures deposited in the Protein Data Bank, only 1.4% is of a membrane protein. Out of these, only a third are unique structures [5, 6]. In light of these difficulties, the structure of a new type of membrane protein is still a remarkable achievement and often renders a publication in the most highly ranked scientific journals.

1.2 AQUAPORINS

1.2.1 DISCOVERY

Historically, it has been a matter of debate whether water cross biological membranes by simple diffusion directly through the lipid bilayer, or if it is conducted through some kind of pore. In the 1970:s, evidence gathered that water passed through membranes via specific protein channels [7, 8]. Through measurements on red blood cells, Macey and co-workers concluded that water transport could not be mediated by diffusion through membranes only and that the transport pore transmitted water in a single file while excluding small solutes or anions. A key experiment that indicated protein mediated transport was the possibility to inhibit water transport with mercurial compounds [7]. However, it was not until 1992 that Peter Agre identified the responsible protein, a contaminant found while searching for Rh antigens in red blood cells. An illustrative proof of the function of this protein was given when oocytes expressing them burst in response to an osmotic chock [9, 10]. The newly discovered water channel was named CHIP28. It was also noted that the protein was homologous to the major intrinsic protein from bovine lens (MIP) that had been studied earlier [11]. The new protein family, of which more members soon were discovered, was later named aquaporins and its first member, CHIP28 was renamed AQP1 [12]. In 2002 the discovery of aquaporins gave Peter Agre the Noble Prize in Chemistry.

1.2.2 OVERALL STRUCTURE AND FUNCTION

The first high resolution structures of aquaporins were reported during the first year of the new millennium [13, 14] (Table 1). Already before that, it had been established through e.g. hydropathy analyses and low resolution electron microscopy images that aquaporins assembled as tetramers, where each protomer contained six transmembrane helices with both

termini on the intracellular side [15, 16]. The protein sequence in the first and second half of the protein seemed to be the result of a gene duplication event. As a consequence, the extracellular and intracellular half of the protein should be related by a twofold pseudo-symmetry axis. Furthermore, the well conserved NPA-motif in loops B and E was thought to meet in the middle of the membrane bilayer to form a narrow region where only water could pass. This model is referred to as the hourglass model [17].

These predictions were confirmed by electron and X-ray diffraction structures at progressively higher resolution (Table 1, Figure 2). From early low resolution studies, it was seen that the transmembrane helices formed a right-handed helical bundle [18] which creates a narrow pore with widening vestibules on each side of the membrane. In addition, two short helices spanning half the membrane from each side were observed. As was later confirmed, these contained the NPA motifs (Figure 3). When atomic resolution data became available, details of the fold could be discerned. A water molecule that is to be transported through the membrane has to pass a narrow tube of about 20Å in length. The diameter is only a couple of Ångströms which means only molecules traversing in a single file can fit. The nature of this pore is amphiphatic, with the carbonyl oxygens from the non-helical part of loops B and E forming a ladder of interaction sites for the water molecules. The remaining wall of the pore is formed by aliphatic side chains of neighbouring helices.

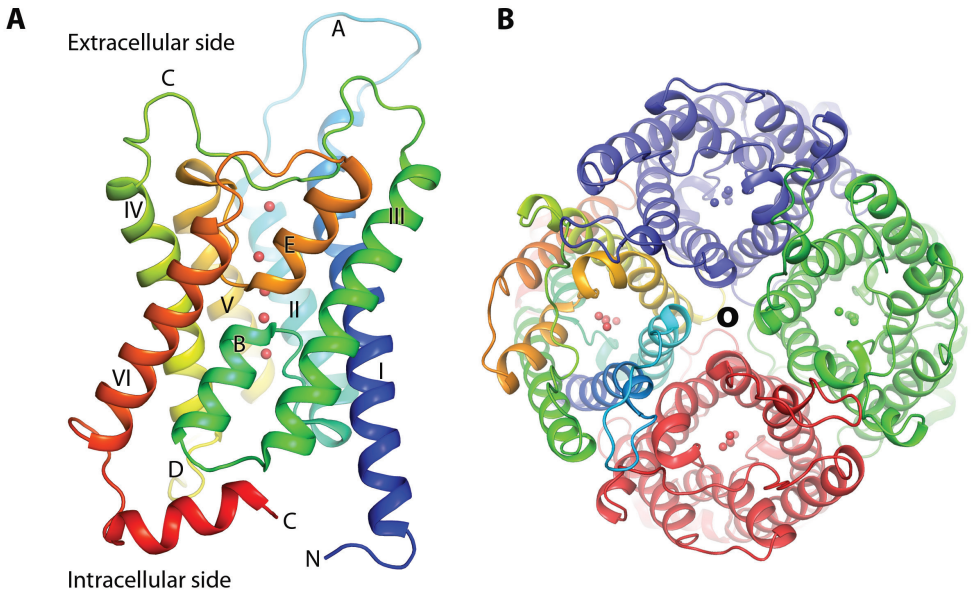

Figure 2. Overview of the AQP fold, exemplified by BtAQP1. The colouring goes from blue (N-terminus) to red (C-terminus). Water molecules in the channel are shown as red spheres. A) Side-view of the protomer with helices and loops labelled with their standard numbering. B) The tetrameric assembly from the extracellular side. The pore formed by the tetramer is marked with o.

A particularly intriguing question is how the two main types of the aquaporin family – the orthodox aquaporins only transporting water and the aquaglyceroporins, also transporting

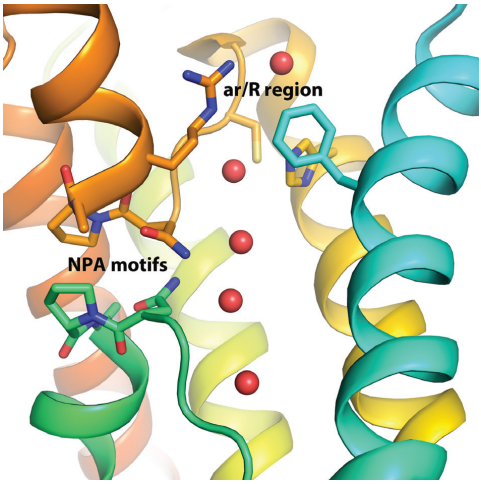

Figure 3. The water conducting channel of AQP1 with key residues shown in sticks. The NPA motifs of loop B and E meet in the middle. Slightly above this, the residues of the ar/R region form the pore constriction. Colouring as in Figure 2.

glycerol and sometimes other solutes – gain their selectivity. The answer lies within the constriction region close to the extracellular surface (Figure 3). Through comparison of structures of water specific [19], glycerol-specific [14] and combined channels [20, 21], it can be concluded that in aquaglyceroporins, this region is wider (~3.4Å as compared to ~2.2Å in water specific channels [22]) and more hydrophobic. This constriction region is often referred to as the ar/R region (for aromatic residue/arginine) due to its amino acid composition. Thus, glycerol is excluded from water channels by its size, while the increased desolvation energy for water prevents its passage through glycerol channels.

A second enigma of aquaporins is how proton translocation is avoided. Since maintaining proton gradients is fundamental for energy generation in any organism, their unregulated transport must be prevented. Protons can be transferred either by direct transport of hydronium or hydroxide ions, or through the Grotthuss mechanism where protons hop from one water molecule to another in a hydrogen bond network. Initially, it was thought that the capture of water molecules in a non-hydrogen bonding orientation by the asparagines in the NPA motif (Figure 3) was the key feature [13]. Later, molecular dynamics simulations and mutational studies led to the conclusion that the electrostatic energy barrier introduced by the dipole moment of the half helices is the main cause [23] but the importance of dehydration penalties [24] and the ar/R region has also been stressed [25].

Table 1. All aquaporins structures solved to at least 4Å resolution.

Protein	Organism	Method	Resol-ution	PDB	Reference	Year
AQP0	Bovine	X-ray	2.24Å	1YMG	[26]	2004
AQP0	Sheep	EM	3.00Å	1SOR	[27]	2004
AQP0	Sheep	EM	1.90Å	2B6O	[28]	2005
AQP0	Sheep	EM	2.50Å	3M9I	[29]	2010
AQP1	Human	EM	3.80Å	1FQY	[13]	2000
AQP1	Bovine	X-ray	2.20Å	1J4N	[19]	2001
AQP1	Human	EM	3.70Å	1IH5	[30]	2001
AQP1	Human	EM	3.50Å	1H61	[31]	2001
AQP2	Human	X-ray	2.95Å		This thesis	2013
AQP4	Human	X-ray	1.80Å	3GD8	[32]	2009
AQP4	Rat	EM	3.20Å	2D57	[33]	2005
AQP4 S180D	Rat	EM	2.80Å	2ZZ9	[34]	2009
AQP5	Human	X-ray	2.00Å	3D9S	[35]	2008
SoPIP2;1	Spinach	X-ray	2.10Å 3.90Å	1Z98 2B5F	[36]	2006
SoPIP2;1 S115E S274E S115E/ S274E	Spinach	X-ray	2.30Å 2.05Å 2.95Å	3CLL 3CN5 3CN6	[37]	2009
AQY1	Pichia pastoris	X-ray	1.15Å 1.40Å	2W2E 2W1P	[38]	2009
PfAQP	Plasmodium falciparum	X-ray	2.05Å	3C02	[21]	2008
AQPM	Methanothermo-bacter marbugensis (archea)	X-ray	1.68Å 2.30Å	2F2B 2EVU	[20]	2005
AQPZ	E. Coli	X-ray	2.50Å	1RC2	[39]	2003
AQPZ	E. Coli	X-ray	3.20Å	2ABM	[40]	2006
AQPZ L170C T183C	E. Coli	X-ray	2.30Å 2.55Å 1.90Å 2.20Å	2O9D 2O9E 2O9F 2O9G	[41]	2007
AQPZ	E. Coli	X-ray	2.40Å	3NK5	[22]	2010
GlpF	E. Coli	X-ray	2.20Å	1FX8	[14]	2000
GlpF wt W84F/ F200T	E. Coli	X-ray	2.70Å 2.10Å	1LDI 1LDF	[42]	2002

1.3 SCOPE OF THE THESIS

Proteins are minute machines that perform the numerous tasks that are needed to make life work, and X-ray crystallography is one of very few tools that provide snapshots from the protein world at the required atomic resolution. Together with methods that characterize these molecules functionally, new insights can be gained about our basic biology. A prerequisite is that the protein chosen for study is available in sufficient amounts in a pure and homogenous from, and the experimental route to achieve this is a science in itself.

This thesis has used these strategies to increase our knowledge about how the protein water channels known as aquaporins function. Aquaporins from two different source organisms and kingdoms of life, human and spinach, has been studied.

SoPIP2;1 is a well studied plant aquaporin from spinach that can open and close in response to environmental changes. This thesis has investigated this water transport regulation through X-ray crystal structures and functional assays in proteoliposomes. In **Paper I**, phosphomimicking mutants showed that opening of the channel is coupled to rearrangements in the N-terminus. We also identified a new potential phosphorylation site with implications for gating. Changes in pH is a physiologically very relevant signal, and in **Paper II**, we could for the first time present structural evidence for how low pH closes the SoPIP2;1 channel. In **Paper III**, the activating effect on SoPIP2;1 of mercury, a compound commonly used as an aquaporin blocker, is structurally and functionally investigated. It is speculated that the observed increase in water transport is triggered by mechanosensitive gating, resulting from mercury's stiffening effect on lipid bilayers. Finally, in addition to a previously identified cadmium binding site in SoPIP2;1 thought to bind calcium *in vivo*, a second similar site is identified with a possible role in gating.

In **Paper IV**, a 2.95Å structure of human Aquaporin 2 is presented, which show that AQP2 is markedly different also from its most closely related homologues. These differences are mainly focused on loop D and the C-terminus and can be related to binding of Cd^{2+} in the structure. We present data that Cd^{2+} could correspond to Ca^{2+} in vivo, and discuss the role of the C-terminal helix as a protein interaction partner. In addition, mutations leading to nephrogenic diabetes insipidus are studied in the structural context.

2 Methods

2.1 THE PATH TO STRUCTURE

The experimental road that leads all the way from a biological question about a protein to the structural and functional data that answers it is often long and winding. It includes several hurdles which not seldom prove to be too high to overcome wherefore a new approach must be tried. Apart from the few lucky cases where a natural source contains large enough quantities of the desired protein to be directly used, experimental procedures must be designed to achieve this.

2.1.1 CLONING

Every protein is coded for by a gene. With modern PCR methods, a gene can be designed to contain basically any desired feature. It is common procedure to include DNA sequences that code for purification tags, protease digestion sites or signal sequences. Furthermore, specific mutations, insertions or deletions in the original proteins are often desirable since they are biologically interesting to study or because they will help overcoming one of the hurdles later in the process. Virtually every protein construct used in this thesis contains a histidine tag and a digestion site to aid purification. In addition, there were many point mutations made for SoPIP2;1 and hAQP2 was codon optimized as well as C-terminally truncated to increase production levels and improve crystallization properties.

Once the gene has been successfully created using a suitable PCR method it is cut-and-pasted into a vector using restriction enzymes. The vector contains all necessary features to express the protein within the production host. This includes a promoter at the optimal length from the gene and selective markers to select for and maintain the vector within the host after transformation. Once the plasmid is taken up by the host, it must be evaluated if the overproduction work as intended before further experiments can take place.

2.1.2 OVERPRODUCTION

The most important feature of an overproduction host is that reasonable amounts of functional protein can be recovered from it. The expression of a membrane protein involves transcription, translation by the ribosome, membrane insertion by the translocon, folding and other post-translational modifications. There are, sometimes very subtle, differences between organisms in how these steps are performed, and how well the needs of a certain protein are matched by the features of the host affects the result tremendously [43]. The knowledge about these factors is yet too shallow to predict the outcome in a specific case, but similarity between the expression host and the source organism increases the likelihood of success. Consequently, a eukaryotic host is usually best for a eukaryotic protein [44]. At the same time, the work effort and costs associated with production increases with the complexity of the host, wherefore the simplest organism that gives a satisfactory result is the method of choice.

2.1.2.1 Pichia pastoris

In this thesis, the budding yeast *Pichia pastoris* has been used for protein overproduction. *P. pastoris*, has emerged as one of the most successful overproduction hosts for eukaryotic membrane proteins and is the dominating expression source for overexpressed membrane proteins that has been structurally determined [6, 45]. Its advantage lies in the tightly regulated alcohol oxidase (AOX1) promoter that is used to drive protein production when *P. pastoris* uses methanol as a carbon source. Furthermore, *P. pastoris* prefers to grow aerobically, which means that it produces biomass instead of toxic fermentation products like ethanol and acetic acid which could otherwise limit the growth [46]. This means that large cell-densities can be achieved, a property that should not be underestimated for low expressing membrane proteins as it increases the amount of cells that can be grown with the same work effort, especially when fermenters are used instead of shaking flasks. Fermenters give the opportunity to control factors such as aeration, pH, temperature and feed levels. As a result, more protein per cell can be produced by fine tuning these conditions for each specific target. A standard production protocol includes a batch phase where *P. pastoris* grows on glycerol, followed by a fed-batch phase where glycerol is supplied in limiting amounts to adapt the cell to starving conditions. Finally, methanol is fed in a limiting manner to induce protein production [47].

For being a eukaryotic host, genetic manipulation of *P. pastoris* straight forward, generation times are short and growth medium cheap. Since the gene of interest is homologically recombined into the genome, expression levels are stable [48]. Posttranslational modifications are often successful even if the details of glycosylation patterns differ from mammalian hosts [47].

2.1.3 PURIFICATION

The overexpressed membrane protein often constitutes less than 0.01% of the material in a cell. For characterization it is essential to have the protein in a pure solution. For membrane proteins, this involves breaking the cells, recovering the membrane fraction, extracting the membrane proteins from the membrane and finally removing all other proteins but the desired one.

2.1.3.1 Solubilization and detergents

While membrane proteins reside in the membrane, most characterization techniques require them to be in solution. However, removing the membrane would expose hydrophobic parts of the protein to the surrounding water, which would lead to collapse of structural integrity and aggregation. The solution is to replace the membrane with detergent molecules. Detergents are surface-active molecules with a hydrophilic headgroup and a hydrophobic tail. At a sufficiently high concentration, called the *critical micelle concentration, CMC*, detergent monomers assemble into roughly spherical micelles where they expose their headgroups to the solvent and hide the tails in the interior. The micelle can cover the hydrophobic part of the membrane protein while keeping it soluble by exposing the headgroups.

The solubilization process starts with accumulation of detergent molecules in the lipid membrane. As the detergent concentration increases, detergents start to interact with each

other and the membrane is split up into small membrane-detergent-protein-fragments that are further delipidated until more or less pure detergent-protein micelles remains [49].

There is a wide range of detergent types and choosing the best one for a particular protein is, as always, a matter of balancing counteracting properties. The detergent needs to efficiently extract the protein from the membrane, but at the same time not denature it. A harsh, efficient detergent often has a charged, small head group and short tail. A mild detergent has the opposite characteristics [50]. The detergent that works best during solubilization might not be the one that is preferred for downstream applications or the one that keeps the protein stable over time. Exchange of detergent after the solubilization step is therefore common. Statistically, maltoside and glucoside detergents have been the most successful in crystallization trials [51]. However, one must remember that researchers tend to use the same substances as has already been successful in other cases, which will make these detergents seem even more superior. A good choice of detergent is one that keeps the protein in a soluble, correctly folded state. But further criteria are important to take into account. Detergents with short carbon tails can be denaturating as the small micelle will not cover the hydrophobic parts of the protein properly. If they work however, they leave a comparatively large area available for forming crystal contacts [50]. A large detergent might cover too much of the protein, shielding also the hydrophilic parts [52, 53], which are very important for forming the stable crystals contacts required for obtaining well diffracting crystals.

In this work, octyl- and nonyl-glucosides have been extensively used for the aquaporins. A newly developed derivate of these, Octyl Glucose-Neopentyl Glycol (OGNPG) [54], was crucial for solving the structure of human aquaporin 2. OGNPG belongs to a new class of amphiphiles that has two carbon chains and two hydrophilic headgroups, all connected via a quaternary carbon atom. This gives extra conformational strain that seems to be favourable for the formation of compact micelles, which decreases CMC and might stabilize the protein-detergent complex [55, 56].

2.1.3.2 Chromatography

All chromatography procedures exploit some feature of the desired protein that makes it different from the contaminants; for example size, charge or affinity towards a ligand. In the modern era of heterologous protein overproduction, the starting point for a standard purification procedure is most often to use a genetically engineered affinity-tag to capture the tagged protein. One of the most common tags is a stretch of histidine residues that bind with high affinity to a resin loaded with divalent cations such as Ni^{2+} or Co^{2+}. The number of histidines has classically been six, but can be increased in cases were binding is inefficient which is often the case for membrane proteins. For hAQP2, it was very beneficial to increase the number to eight.

The protein is often fairly pure already after the affinity step. However, a gel filtration step is usually included as a last step in the purification protocol. Apart from polishing the purity, gel filtration offers the possibility to change the buffer and/or detergent and is also an important quality check. Even if everything seem well after the initial purification step, evidence of aggregated or inhomogenic protein can be revealed by gel filtration. This is a

strong indication that the protein might not perform well in later applications, especially not in crystallization.

Other chromatography techniques are ion-exchange and hydrophobic interaction chromatography where proteins bind the column material with different affinities depending on their surface charge or hydrophobicity, respectively. These can be included as extra steps if the achieved purity is not enough, or if there is no affinity tag to exploit. However, care should be taken not to over-purify the protein. Proteins often bind cofactors that are vital for their function and/or stability that might be removed by extensive purification. Especially for membrane proteins, structurally important lipids might be removed, which can be detrimental to any crystallization attempt [53].

2.2 X-RAY CRYSTALLOGRAPHY

In the early 1600:s, humans started to develop microscopes, which made it possible to explore the world not visible to the naked eye. The components of blood, microorganisms and details of insects were reported for the first time. As the technology developed, finer and finer details could be resolved. However, the resolution for a light microscope is limited by the wavelength of visible light, and no matter how skilfully the microscope is constructed, it will never reach beyond 200 nanometres. In our days, science wants to answer questions about the smallest building blocks constituting living organisms. This requires full atomic resolution, which means that it must be possible to discern objects only about 1 Ångström apart. One way this can be achieved is through X-ray diffraction. But before the X-ray diffraction experiment can take place, crystals must be formed.

2.2.1 CRYSTALS

A crystal is the arrangement of a large number of identical molecules in a defined, repeating pattern. The smallest repeating unit of the crystal is the *asymmetric unit*. By applying a set of symmetry rules, such as rotation or mirroring, the whole *unit cell* can be generated, which contains a handful of molecules, the exact number of which is specific for the given arrangement. There is a finite number of ways in which the molecules can be arranged, and each unique packing pattern is referred to as a *space group*. The total number of space groups is 230, however only 65 of them are possible for a protein since it is a chiral molecule that cannot crystallize with any symmetry elements based on mirroring. The unit cell is in turn repeated translationally throughout the crystal in all three dimensions.

2.2.2 CRYSTALLIZATION

The goal of a crystallization experiment is to persuade the individual molecules to arrange in the repetitive arrangement of a crystal. Several methods exist for this, the most common being vapour diffusion which is what has been used in this thesis. In the basic experiment, a small droplet, often less that 1 μL, of highly concentrated protein is mixed with an equally sized droplet of precipitant solution, containing a mixture of chemicals thought to be beneficial for crystal formation. This mixed droplet is then put in a sealed container containing a large reservoir of precipitant solution (Figure 4A). Since the crystallization drop

is diluted compared to the pure precipitant solution, water will start to evaporate from the drop to the reservoir. The idea is to slowly go from a state where the protein is in solution into the supersaturated state. This state has several zones (Figure 4B). If water is withdrawn from the drop too quickly, disordered protein aggregates will form in the precipitation zone. In the metastable zone, the solution is not saturated enough to start crystal formation. The desirable state is the nucleation zone. A nucleus is the starting point of a crystal where a handful of molecules have assembled. When a protein molecule is incorporated into the crystal, it leaves the solution and goes into the solid state. Consequently, the solution as a whole is no longer supersaturated and crystal formation is halted until further water has evaporated and the supersaturated state is reached again. In a successful crystallization experiment, only a few nuclei are formed in the initial state and then slowly grows into large, well-ordered crystal as the state of the crystallization drop follows the supersaturation phase line [57].

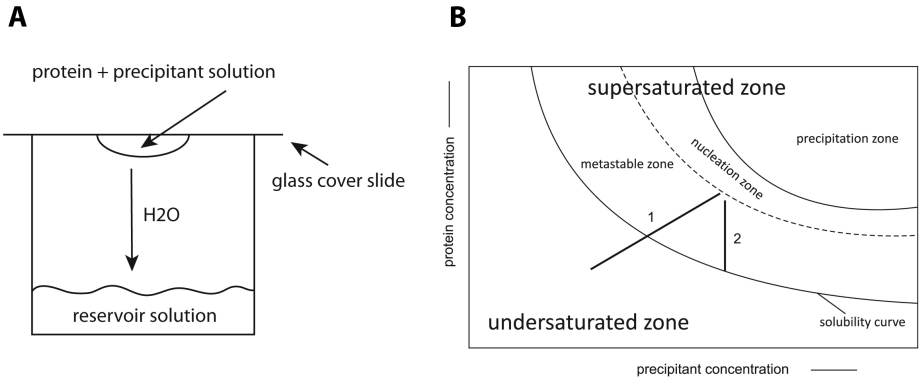

Figure 4. A) Schematic of a hanging drop vapour diffusion crystallization experiment. B) Phase diagram showing the different zones involved in crystal formation.

Since crystallization usually does not come natural for a protein, great care must be taken to create the right environment. A too brutal phase transition will result in unordered protein aggregates to form. Likewise, a too low precipitant concentration will not result in any crystal formation at all. It is also common to achieve crystal formation, but since so many nuclei are formed, hundreds or thousands of small crystals are formed instead of a few large. Despite many efforts to rationalize the crystallization procedure, it still remains a handicraft that requires skill and experience of the scientist.

The precipitant solution usually contains one major precipitant which may be a salt, but more commonly for membrane proteins some type of polyethylene glycol [51]. In addition, buffers, other salts, solvent, detergents or other molecules are added to improve the crystallization conditions in an iterative process where the crystal appearance and diffraction properties are used as a guide.

Apart from vapour diffusion, crystallization techniques which try to mimic the lipid environment of membrane proteins exist. These include the lipidic cubic phase [58], sponge

phase [59] and bicelle methods [60]. The proteins are still detergent solubilized during the purification process, but are returned to a bilayer environment in the crystallization experiment.

The likelihood of success for a crystallization trial is heavily dependent on the molecules ability to form specific interactions that will create the highly ordered crystal structure. A heterogeneous sample or a sample that only has a small area with defined structure exposed is more likely to fail. The large transmembrane, hydrophobic surface of membrane proteins are covered by the irregularly shaped detergent micelle which leaves only the hydrophilic end domains available for crystal contacts. Thus the resulting crystals, if any, have a high solvent content and are kept together by very few interactions. The result is small, weakly diffracting crystals of low quality. A first step to improve the protein properties in this respect is to remove flexible parts of the protein that might interfere with crystal packing. This was done successfully for AQP2 in this thesis. More drastic routes to circumvent these difficulties are to use antibodies or nanobodies to create crystal contacts and lock proteins in defined conformations [61, 62]. Another strategy is to genetically insert a small protein with good crystallization properties in a loop region to improve the crystallizability [63].

2.2.2.1 Cryoprotection of crystals

When a crystal is found it needs to be tested for diffraction. This requires the crystal to be fished from the drop and mounted in an X-ray source. Earlier in the history of protein crystallography, crystals were being exposed to X-rays in room temperature, which leads to fast destruction of the crystals due to radiation damage. As a result, data had to be combined from many crystals to solve the structure. Nowadays, it is common procedure to freeze the crystals in liquid nitrogen which often makes it possible to collect a complete dataset from one crystal also when using intense synchrotron sources. However, freezing a crystal is not a simple issue. A protein crystal contains large amounts of water which upon freezing transform to crystalline ice that destroy the crystal due to the volume increase. To prevent this, cryoprotectants must be added which delays the ice formation process so that water is trapped in the glass-state. Common substances are glycerol or short polyethylene glycols, e.g. PEG400. Non-optimal cryoprotectants might dissolve the crystal or give it a severe osmotic chock, which will destroy its diffraction properties. Thus, the establishment of a good cryoprotocol can be a very painstaking process and the order in the frozen crystal will always be somewhat worse than in the unfrozen state [64].

2.2.3 X-RAY DIFFRACTION

Diffraction is generally defined as the bending of waves when it encounters an obstacle or passes through a slit that is of similar magnitude as their wavelength. X-rays with a wavelength of about 1Å are thus ideal for studying the atomic details of molecules. In theory, the scattering of X-rays by a single molecule should be enough to reconstruct its structure, but the diffraction of a single object is much too weak to be detected. If many identical objects are arranged together in a regular fashion, as in a crystal, they will all scatter the wave. In most directions, the waves will cancel each other out, but in some positions, defined by Bragg's law;

$$n\lambda = 2dsin\theta$$ *(Equation 1)*

they will reinforce each other and result in a diffraction pattern consisting of defined spots. The position of these spots is a consequence of the crystal packing, while the intensities of the spots contain information about the atomic arrangement in the molecule. Every diffraction spot has an index *hkl* and has a specific amplitude and phase. This is called a structure factor, $\mathbf{F}_{hkl}$. The aim of a diffraction experiment is to measure as many diffraction spots as possible and determine their position and intensity. This information can then contribute to solving the three-dimensional structure of the molecule that built up the crystal.

The part of the atoms that the X-rays interfere with is the electron cloud. Thus, the resulting image will represent the presence of electrons. The electron density ρ at the position xyz, can be calculated according to

$$\rho(x\ y\ z) = \frac{1}{V}\sum_{h}\sum_{k}\sum_{l} |F_{hkl}| \exp\ [-2\pi i(hx + ky + lz) + i\alpha(h\ k\ l)] \quad \textit{(Equation 2)}$$

which is a summation over all structure factors *hkl*.

2.2.3.1 The phase problem

However, one big obstacle remains. A wave is defined both by its amplitude $|F_{hkl}|$, and its phase α (Equation 2), and both are vital to reconstruct the molecule that scattered the wave. The amplitude is preserved in the diffraction spot as the square root of the intensity, but the phase information is lost. This is often referred to as the "Phase Problem of X-ray Crystallography". Several methods exist to solve this. These methods all exploit some clever guessing to get an initial set of phases, which then can be improved in an iterative way. Central in this respect is the Patterson function, a derivation of Equation 2:

$$P(u\ v\ w) = \frac{1}{V}\sum_{h}\sum_{k}\sum_{l} |F_{hkl}|^2\ \cos\ [2\pi(hu + kv + lw)] \quad \textit{(Equation 3)}$$

The Patterson function uses the intensities, F_{hkl}^2, directly and hence does not include the phase term. This means that the electron density cannot be calculated and the position of atoms remain undetermined. What it does describe is the vectors *uvw* between atoms, which can be utilized in a number of ways with the help of the resulting Patterson map.

The most straight forward approach is to use Molecular Replacement. Here, the phase information for a previously determined X-ray structure of a similar molecule is used as a starting point. By trying to overlap the Patterson maps for the known and unknown molecule, the rotational position of the unknown molecule in the unit cell can be determined. This is followed by a translational search to determine the xyz coordinates for the molecule. If this process is successful, the structure is solved.

Molecular replacement obviously requires that structural information from a similar molecule available. If no similar crystal structure has been solved before, one has to turn to methods such as Multiple or Single wavelength Anomalous Dispersion (MAD/SAD) or Multiple Isomorphous Replacement (MIR). All of these methods rely on the presence of heavy atoms in the structure. MAD/SAD uses the small differences in the scattering of heavy atoms at certain wavelengths, whereas in MIR, diffraction data with and without the heavy atoms are compared. If the positions of the heavy atoms can be determined with the help of the Patterson map, the phases of this substructure can be used to reconstruct the phases for the entire molecule.

2.2.3.2 The diffraction experiment

The aim of the diffraction experiment is to accurately measure as many diffractions spots as possible. The typical experiment involves rotating the crystal in the x-ray beam and record an image for every ~0.5° wedge, until all diffraction spots have been covered (Figure 5).

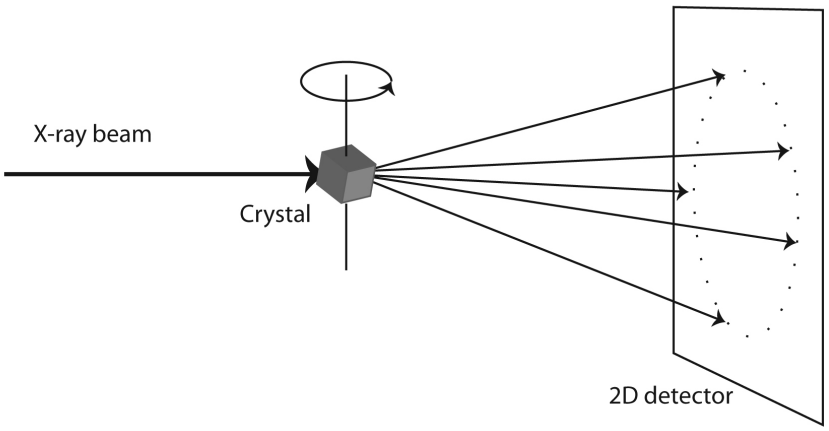

Figure 5. Schematic of the diffraction experiment. The X-rays hit the rotating crystal and the diffraction spots are captured on a detector.

This requires an experimental set-up where a range of factors can be tightly controlled. A modern synchrotron beam line environment is developed for this purpose. This includes a high intensity X-ray beam with low divergence to give sharp spots from weakly diffracting crystals. One very important aspect is to reduce the background to be able to capture the weak high resolution spots. Several hardware features such as detector properties and a beam size that can be matched to the size of the crystal are important in this respect. Other central issues are sample specific properties, such as mosaicity or non-crystalline material around the crystal and experimental settings such as the oscillation range by which the crystal is rotated during each frame.

2.2.3.3 Data processing, refinement and validation

Once the data is collected, it needs to be processed to extract the structural information it contains. This process starts with *indexing* and *integration* where spot positions and intensities

are determined. The next step, *data reduction*, scales the intensities to correct for various experimental factors and compares symmetry related reflections. Once this is done, *phasing* can be attempted using one of the methods mentioned above. After finding an initial set of phases, a model of the protein is fitted into the preliminary electron density. The phases and the model can then be refined in small steps by combining the interpretation of the electron density with knowledge about the geometry of chemical bonds and angles. However, there are many pitfalls in this process, and some kind of quality assessment is necessary. The solution has become to use the crystallographic R-value, which assays how well the structure factor amplitudes of the calculated model describe the observed data according to:

$$R = \frac{\sum_{hkl} \left[|F_{obs}(hkl)| - |F_{calc}(hkl)| \right]}{\sum_{hkl} |F_{obs}(hkl)|} \qquad \textit{(Equation 4)}$$

During the course of the refinement, the R-value should decrease as the model is improving. But there is a risk of modelling noise, which would give a low R-value at the expense of the correctness of the model. This situation can be prevented by also monitoring R_{free} [65], which is calculated as in Equation 4, but using a set of reflections that has not been included in the model calculation. R and R_{free} should follow each other during the refinement process, otherwise it indicates that something is wrong with the chosen strategy.

A further factor to take into the account to ensure scientifically sound result is the geometry of the modelled molecule. There is good knowledge about what angles and bond lengths are allowed in a protein molecule, and if too much attention is paid to the electron density at non-atomic resolution, one can arrive at questionable results. Moreover, model bias can be significant, especially when molecular replacement has been used to acquire the initial phases. This means that the electron density maps might be misleading. Composite omit maps, where an electron density map for the entire structure is put together from small pieces that where calculated without the model for that particular piece, can complement the ordinary maps to relieve this situation.

The map that is most often used to view the electron density is the $2F^{obs}$-F^{calc} map, and this is used in combination with the difference density map F^{obs}-F^{calc}, that highlights features that are absent or wrongly included in the model. The strength of any feature is referred to by their σ-level. For example, in a map displayed at 1σ, the electron density visible is at least one standard deviation above the average of the unit cell.

Once the structure is satisfactorily refined, what remains is to interpret the biological implications of the newly determined protein structure. An overview of the process of going from crystal to structure can be seen in Figure 6.

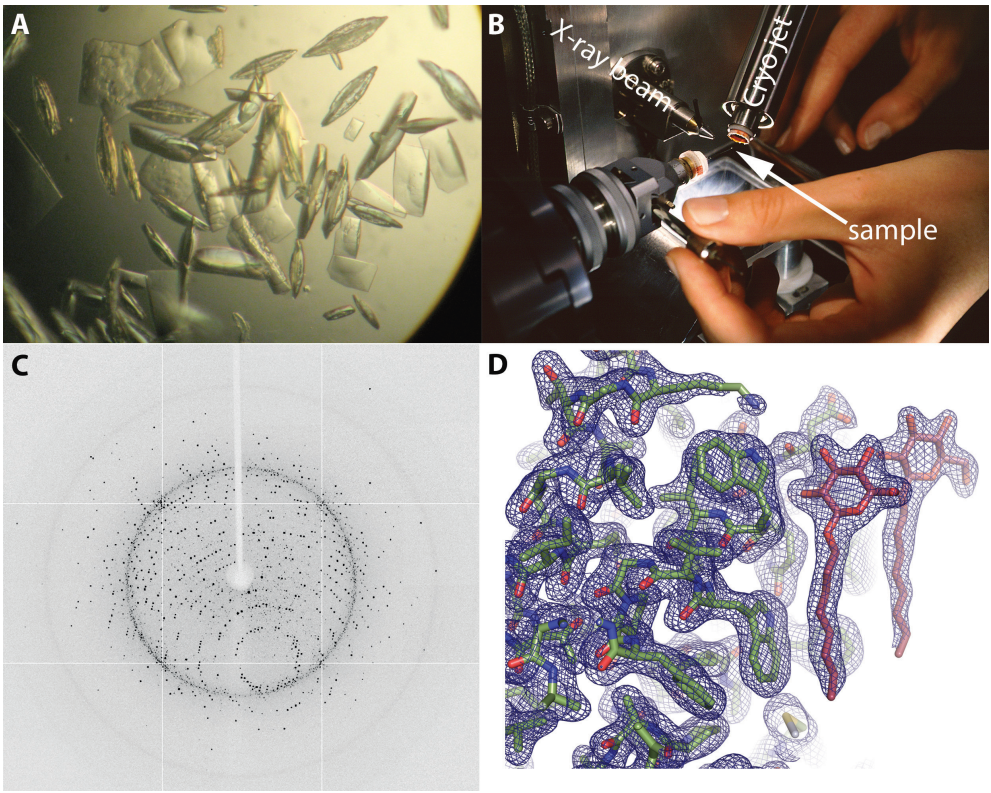

Figure 6. From crystal to structure. Crystals formed in a vapour diffusion drop (A) is mounted in the X-ray beam (B, white arrow), while cooled in liquid nitrogen. Diffraction is recorded (C) and used to calculate the electron density (D, blue mesh) into which the crystallized molecule can be modelled. Crystals, diffraction and structure are from the SoPIP2;1 structure described in Paper III. B: credit Denis Morel (ESRF).

2.2.4 Characterization Techniques

2.2.4.1 Liposomes

Since the function of many membrane proteins is to transport a compound from one side of the membrane to the other, it is necessary to test their functionality in this type of environment. Even if this sometimes can be done on proteins in their natural membrane, results are more easily interpreted if a pure population of the desired protein can be studied. To this end, proteins can be reconstituted into artificial membrane bilayers; liposomes. Unilamellar liposomes can be easily formed by subjecting an aqueous lipid mixture to e.g. sonication or extrusion through a small membrane. To reconstitute a membrane protein into it in a functional, homogenous state is often more of a challenge. Most protocols rely on first destabilizing preformed liposomes with detergent and then adding the protein. Depending on the system, the optimal point can be when the liposomes are intact but saturated with detergent, or when the liposomes have been completely solubilized into mixed lipid-detergent-protein micelles. The degree of destabilization can affect the quality of

proteoliposomes and whether the proteins are unidirectionally inserted or randomly oriented in the bilayer [66]. In the next step detergent is removed from the solution and the membrane protein ends up inserted into the lipid bilayer. Detergent can be removed by e.g. dialysis or dilution. This works well for detergents with high CMC, but is more difficult when CMC is low as this requires a more thorough elimination. In these cases, adsorption on polystyrene beads is a preferred method [67].

2.2.4.2 Stopped-flow spectroscopy

Stopped-flow spectroscopy is a method for fast mixing of small volumes while monitoring spectroscopic changes in the sample. Rapid mixing is crucial when studying fast processes to minimize the dead time before data can be acquired. Usually, the dead time is in the order of milliseconds.

In this thesis, stopped-flow spectroscopy has been used to assay water transport rates of aquaporins reconstituted into liposomes (Paper I and III). When proteoliposomes are subjected to an osmotic chock, water will leave or enter the liposomes depending on the applied osmotic gradient. The volume change of the liposomes affects their light scattering properties. The change in the amplitude of light scattering can be mathematically described with a differential equation, the solution of which can be approximated with an exponential function:

$$y = A_1 e^{-kt} + A_2 \qquad \textit{(Equation 5)}$$

The k-value of this function can be extracted from the curve fitting analysis and used to calculate the osmotic permeability constant P_f according to:

$$P_f = \frac{k\,(1 - \frac{b}{V_0})}{\frac{S}{V_0} * V_w * c_{out}} \qquad \textit{(Equation 6)}$$

where S is the surface area and V_0 the initial volume of the vesicle, b is the osmotically inactive vesicle volume, V_w is the partial molar volume of water and c_{out} is the osmolality on the outside of the vesicles [68].

In practise, the proteoliposome solution is mixed with a hyperosmotic solution, containing a non-permeable solute such as sorbitol or sucrose. As a result, water leaves the liposomes, resulting in shrinking and increase of light scattering. The reconstitution process sometimes leaves some liposomes empty. The shrinkage of the resulting mixed population often makes it necessary to use a double exponential function instead of Equation 5.

3 Plant Aquaporins

Plants depend on water for many aspects of their physiology. Water loss through transpiration and water uptake through roots are situations where plant aquaporins are important, but roles are also suggested in cell expansion, nutrition uptake and plant reproduction [69]. Since plants have to cope with environmental changes where they happen to grow, the precise regulation of water transport in and out of the cell is fundamental. Furthermore, the extensive compartmentalization of plant cells requires elaborate fine tuning also internally [70]. This is reflected in the large number of isoforms within the same plant species; 35 in *Arabidopsis thaliana* [71] and 33 in rice [72], compared to 13 in humans. In addition, plant aquaporins often respond to environmental stress by regulating the water transport through individual water pores by gating. Plant aquaporins have been shown to be gated by phosphorylation, pH and Ca^{2+}.

3.1 TYPES

Historically, plant aquaporins have been divided into four subfamilies; Plasma Membrane Intrinsic Proteins (PIP), Tonoplast Intrinsic Proteins (TIP:s), Nodulin26-like Intrinsic Proteins (NIP:s) and Small Basic Intrinsic Proteins (SIP:s) [71]. However, recent investigations has complicated the picture by identifying further isoforms (GlpF-like Intrinsic Proteins, X Intrinsic Proteins and Hybrid Intrinsic Proteins) [73], and also showing that the distribution within the plant cell of the previously known classes is not as uniform as implied by their names [74]. Aquaporins are found in the plasma membrane as well as in intracellular compartments such as the tonoplast membrane of the vacuole (TIP:s and PIP:s), chloroplasts (TIP:s and PIP:s), endosomes (TIP:s and PIP:s), and ER (SIP:s and NIP:s) [74]. Apart from water, different isoforms have been shown to transport glycerol, urea, hydrogen peroxide, boric and silicic acid, ammonia and carbon dioxide [69, 75].

The plant aquaporin studied in this thesis, SoPIP2;1 from spinach (*Spinacia oleracea*), is a member of the PIP subfamily and is highly abundant in the plasma membrane of spinach leaves [76]. PIP:s can be divided into two sub-classes, PIP1 and PIP2, the main differences lying in the shorter N-terminus and longer C-terminus of the PIP2 isoform [77]. The topology of SoPIP2;1 is shown in Figure 7. PIP2:s are much more efficient water transporters compared to PIP1:s, and it has been shown that co-expression of PIP1:s and PIP2:s is required to avoid retaining PIP1:s in the ER, and that the two isoforms form heterotetramers [78, 79].

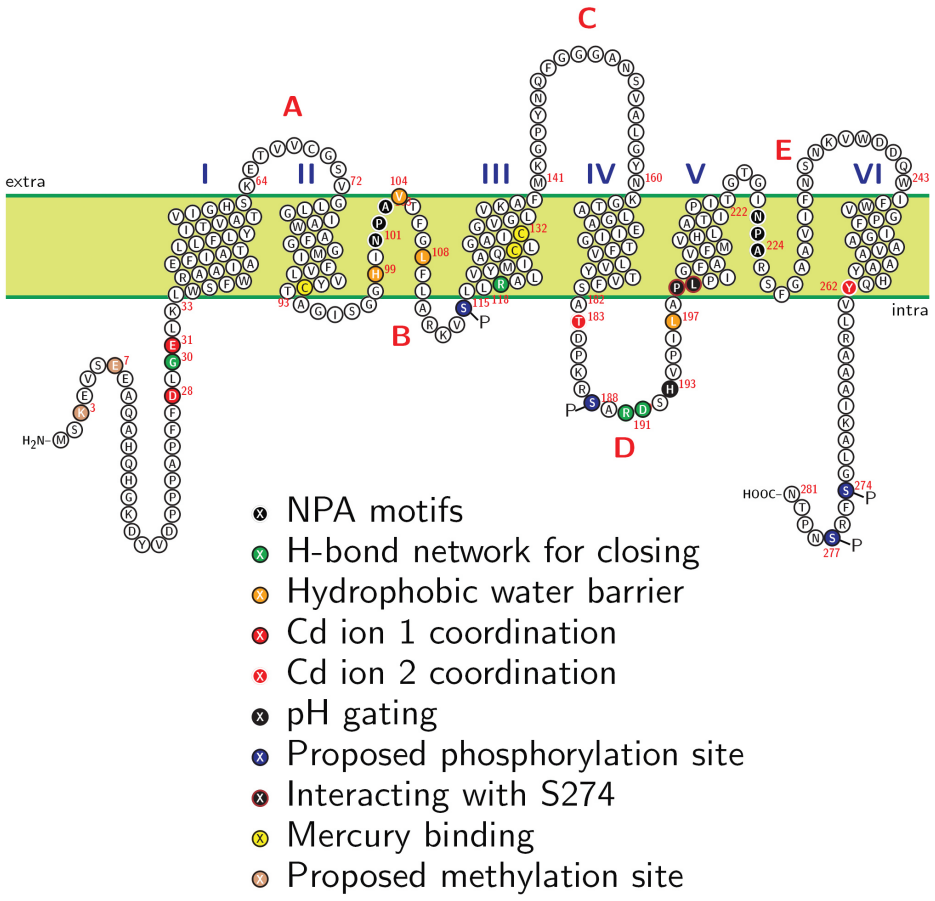

Figure 7. The topology of SoPIP2;1 with some residues relevant in this thesis highlighted.

3.2 Regulation (Paper I-III)

SoPIP2;1 is to date the only structurally determined plant aquaporin and has provided a structural framework for plant aquaporin gating. From the initial structures in both open and closed conformations [36], the structural mechanism for gating by phosphorylation, divalent cations and pH could be explained. The key aspect of the gated plant aquaporins is the extended loop D which in the closed state serves as a cap for the water conducting channel (Figure 8A). In the closed structure at 2.1Å, the conserved Leu 197, situated at the border between loop D and TM5 is inserted into the channel. Together with a few other aliphatic amino acids, this residue creates a hydrophobic barrier. The closed conformation is stabilized by anchoring loop D to the N-terminus via loop B, water molecules and a Cd^{2+} binding site (Figure 8B). Specifically, Asp 28 and Glu 31 are coordinating the metal ion and a connection is made to Arg 118 in loop B. This residue, and Gly 30 in the N-terminus, interacts with

Arg 190 and Asp 191 of loop D through water molecules. Several lines of evidence indicate that these interactions are relevant for the situation in the plant. As is discussed further below, there is convincing evidence that Ca^{2+} takes the role of the Cd^{2+} ion *in vivo* [80, 81]. The key residues, Asp 28, Glu 31 and Arg 118 are all well conserved within the PIP family and functional data confirms their role for the gating mechanism [36, 82].

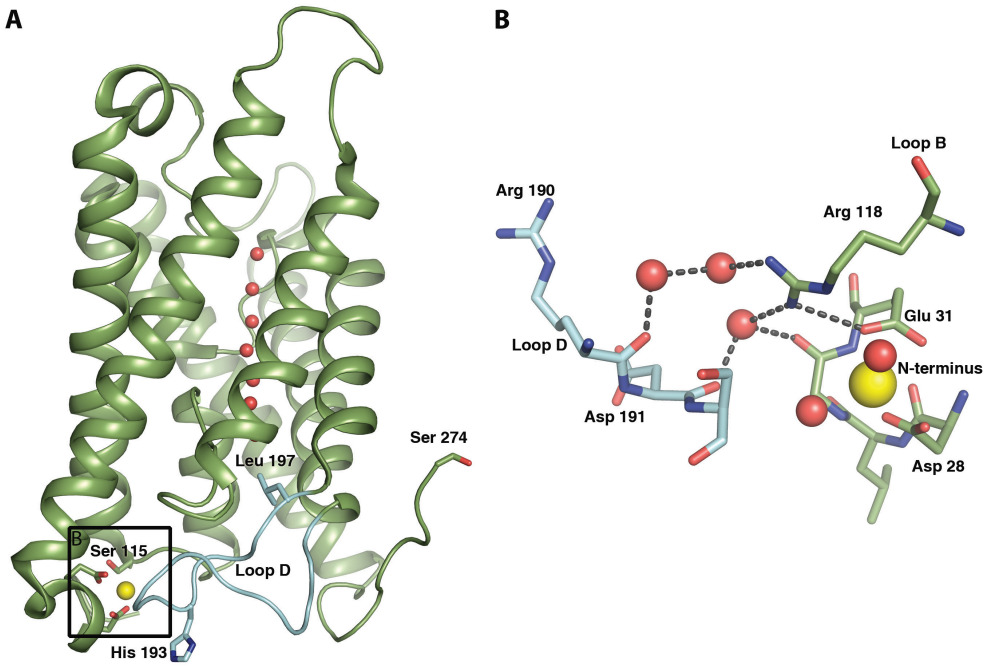

Figure 8. The structural elements involved in gating of SoPIP2;1. A) Overview of the protomer. Loop D is highlighted in blue. The Cd ion and water molecules are represented by yellow and red spheres, respectively. B) Detailed picture of the interactions anchoring loop D to the N-terminus.

The open structure of SoPIP2;1 lacks Cd^{2+} and loop D has swung away. TM5 is extended a further half turn into the cytoplasm, removing Leu 197 from its blocking position in the channel. The resolution is considerably lower (3.9Å) compared to the closed structure, but the change of conformation is clear.

In this thesis, new crystal structures and functional assays has shed further light on the mechanism of the gating of SoPIP2;1 by pH and phosphorylation. In addition, new insights has been gained into the effect of mercury, a traditional aquaporin inhibitor which in the case of SoPIP2;1 was seen to have an activating effect.

3.2.1 POSTTRANSLATIONAL MODIFICATIONS

3.2.1.1 Gating by phosphorylation (Paper I)

From a gating perspective, phosphorylation of a completely conserved serine in loop B and a serine in the C-terminus have been the most thoroughly discussed. In SoPIP2;1, these amino

acids are Ser 115 and Ser 274. Making Ser 115 unphosphorylatable by an S115A mutation decreases the water transport rate in *Xenopus* oocytes for SoPIP2;1 [83], ZmPIP2;1 [84] and PvTIP3;1 [85]. This site lies within in a consensus site for several types of kinases and is conserved in all PIP:s [83]. In the case of SoPIP2;1, kinase inhibitors seemed to prevent phosphorylation in oocytes, as the water transport rate by the wild-type was affected by this treatment, but not S115A [83]. However, direct evidence of phosphorylation at this site in planta has never been shown. Still, increased phosphorylation of this site in maize protoplasts correlated with increased water conductance in response to chilling stress, as detected by a specific antibody [86]. Specifically for SoPIP2;1, increased phosphorylation of a Ser 115-containing peptide was detected when using kinases isolated from spinach leaves [87].

By contrast, there is extensive evidence for the phosphorylation of Ser 274 when studied in the plant. Phosphorylation has been detected here for PIP2:s in *A. thaliana* [88, 89], maize [84], spinach [83], broccoli [90] as well as in soybean NIP [91]. This site is conserved among PIP2:s and some NIP:s, and the kinase responsible has been partly purified in spinach [87]. When examined in oocytes, a S274A mutant from common ice plant had partly abolished water transport ability in oocytes [92], and in SoPIP2;1 water transport increased upon treatment with phosphatase inhibitors only for mutants still containing this phosphorylation site [83]. However for maize ZmPIP2;1, mutating this site to alanine or glutamate did not affect the phenotype in oocytes [83, 84], and S274A had the same basic water transport rate as wild-type for SoPIP2;1 [83].

Mechanistically, a role for both Ser 115 and Ser 274 can be seen in the closed X-ray structure [36]. Ser 115 is occupying a key position and phosphorylation of this residue would disturb the interaction between the N-terminus and loop D, thus opening the channel. This was also observed in molecular dynamics simulations, where phosphorylation of Ser 115 triggered the release of loop D, which in turn started its transition towards the open conformation.

The other phosphorylation site at Ser 274 is located at the C-terminus far away from loop D within the same protomer. However, Ser 274 is seen to interact with residues in the beginning of TM5 in a neighbouring protomer, thus stabilizing loop D in the closed conformation. When comparing the open and closed structures, a steric clash is observed between Ser 274 in the closed and Leu197 in the open conformation. Phosphorylation of Ser 274 results in a conformational change of the C-terminus and removal of this steric clash, allowing for loop D to swing open.

To further investigate the mechanism behind gating and hopefully be able to determine a structure of the open conformation to a higher resolution, we set out to structurally and functionally characterize phosphomimicking mutants of SoPIP2;1. An established way of imitating the phosphorylation of a serine residue is to replace it with a larger and negatively charged amino acid, often glutamate. Thus, the S115E, S274E and the corresponding double mutant were constructed. Mutation of Ser 115 to glutamate resulted in a complete disruption of the Cd-binding site and an extension of TM1 into the cytoplasm (Figure 9A). However, although some of the hydrogen bonds between loop D and the N-terminus were broken in both the single and double mutant, the structure remained closed. This was further

supported by the functional data which did not show any significant differences in water transport when compared to wild-type. We proposed that the disruption of the Cd-binding site and the resulting extension of TM1 together with the similar extension of helix 5 seen in the open structure, would be seen in a truly phosphorylated, open channel.

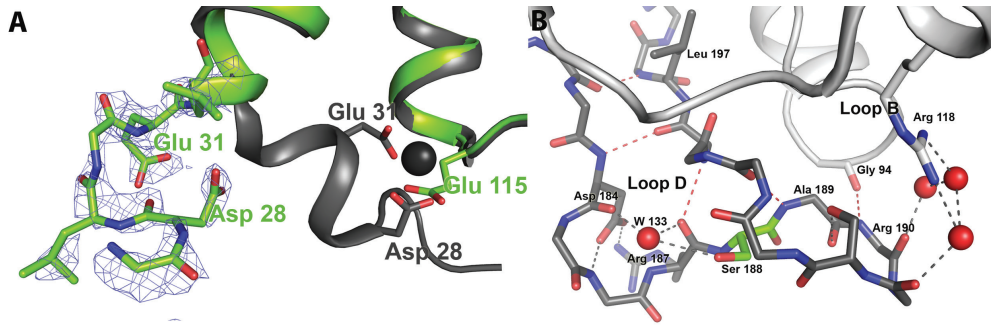

Figure 9. A) In the S115E structure (green) the Cd-binding site is disrupted and the N-terminus has changed conformation compared to the closed wild-type structure (grey). B) Ser 188 is situated at a key position in loop D, and its phosphorylation has the potential of breaking up the hydrogen bond network that keeps loop D together.

Concerning phosphomimicking mutations, a glutamic acid differs from a phosphate group in size and charge, and may not always fully mimic a phosphorylated state [93]. For S115E structure, this seems to be the case as the Cd-binding site is destroyed but the overall conformation is still closed, and the water transport rate is not altered compared to wild-type. In line with this, a calculation of the electrostatic potential for the S115E structure revealed that the negative potential introduced by the glutamate was only half of that for a phosphoserine.

The replacement of Ser 274 with glutamate resulted in a disordered C-terminus as suggested from the wild-type structure, indicating that the steric clash between Ser274 and the Leu197 in the open conformation is removed. However, as for the S115E mutation, this was not enough to open the channel.

In addition to these well studied phosphorylation sites, we noted that Ser 188, a residue in loop D which has a central role in this loops internal H-bonding network (Figure 9B), also lies within a kinase consensus site. The S188E mutation increased the water transport rate in proteoliposomes (Figure 11D), which indicates that mimicking phosphorylation in this position breaks up the integrity of loop D so that it can no longer remain in the closed conformation. This was supported by molecular dynamics simulations, where it was seen that the closed conformation was destabilized when Ser 188 became phosphorylated as interactions were created between loop D and the C-terminus. Phosphorylation *in vivo* at this site has not been investigated, but when studied in oocytes the unphosphorylatable mutant ZmPIP2;1 S203A, was found to have a lower water transport rate than wild-type [84]. This residue is also situated in loop D but four amino acids later in the sequence compared to SoPIP2;1 S188E and might play a similar role.

3.2.1.2 Regulation by other posttranslational modifications

In addition to the phosphorylation sites mentioned above, several other posttranslational modifications of PIP:s have been observed (Figure 7). Members of the PIP2 subfamily are phosphorylated in the plant at the site corresponding to Ser 277 in SoPIP2;1 [88]. This does not affect the water transport properties of the channel, but is instead related to trafficking. In AtPIP2;1, there is also evidence for ubiquitination at an undefined site, leading to degradation. Methylation of an N-terminal lysine and glutamine as well as cleavage of the initial methionine has also been shown, but the physiological role is still unclear [94, 95].

3.2.2 pH (paper II)

The maybe most well studied gating mechanism of plant aquaporins is the one mediated by pH. Flooding causes anoxia, which in turn lowers the pH of the cell [96] and closes the aquaporins through a pH-sensitive gating mechanism [80, 81, 97, 98]. This phenomenon was first studied in *A. thaliana* [99] where it was shown that protonation of a conserved histidine in loop D triggered closure of the PIP:s. In the first structure of SoPIP2; [36], it could be seen that this residue, His 193, was centrally placed with respect to the structural elements important in gating. It was suggested that a protonated rotamer of the histidine could interact with Asp 28 in the N-terminus, keeping loop D in place and capping the water conducting channel (Figure 10A). However, since this structure was determined at pH 8, the proposed interaction, although it seemed likely, could not actually be observed.

In order to verify the proposed mechanism, we solved a structure of SoPIP2;1 at pH 6, just below the pK_a of histidine. At this pH, the flip of the histidine side chain could be observed in one out of four protomers. However, the N-terminus has moved away due to the absence of a divalent cation, and the predicted interaction could not take place (Figure 10B). Instead His 193 was seen to interact with loop B through a water molecule (Figure 10C). The physiological relevance of this would be that pH gating could be achieved also when no Ca^{2+} is present to keep the floppy N-terminus in place, as there is also an opportunity for His 193 to interact with the static loop B (Figure 10D). Likely, the originally postulated mechanism involving the calcium binding site is also in operation. This has been supported by functional analysis of D28A and G31A mutants, which had a reduced pH-sensitivity [82]. In the same study it was seen that the R124A mutant, which removes the arginine that connects loop D to the N-terminus, retains its pH sensitivity, although the cation dependence is lost. A structure of the R124A mutant likely would show that the N-terminus has moved away as its anchoring point is lost and His 193 is out of reach for the N-terminal residues. The remaining pH sensitivity of this mutant further supports our finding that an alternate connection to loop B can stabilize closing due to low pH.

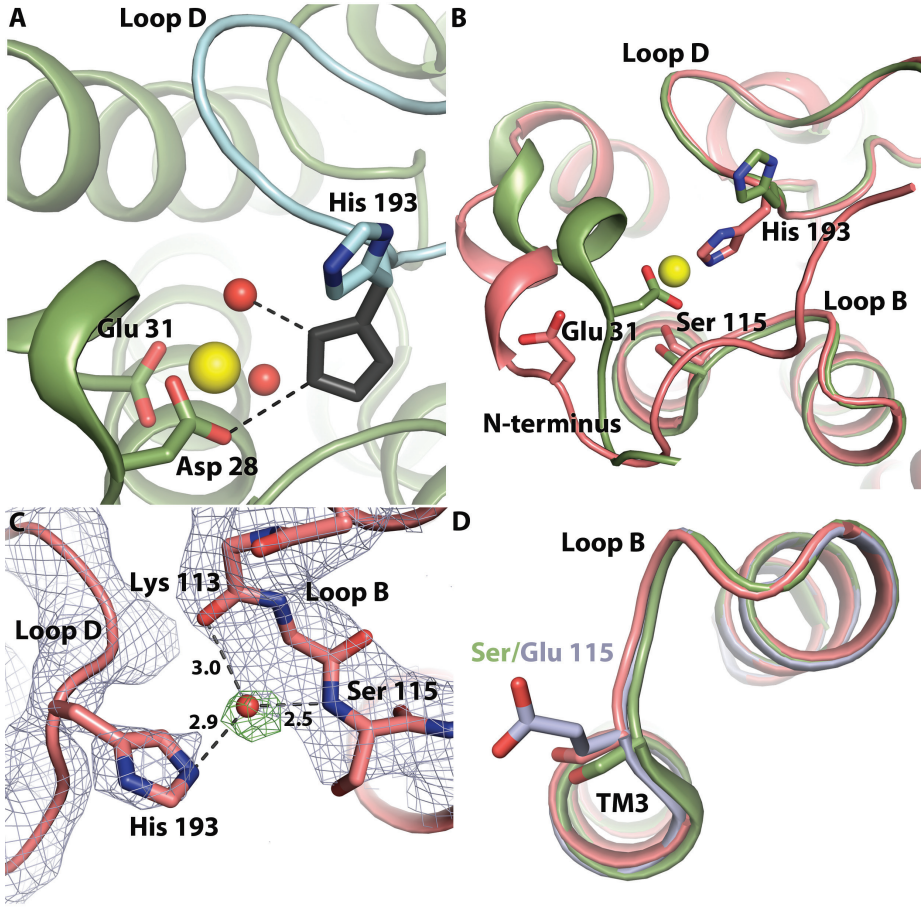

Figure 10. SoPIP2;1 and pH gating. A) In the originally proposed pH gating mechanism, a protonated rotamer (grey) of His 193 in the wild type closed structure at high pH (green) was proposed to interact with Asp 28 to close the channel. B) In the structure at low pH (pink) His 193 has flipped, but the N-terminus has moved away. C) His 193 is instead interacting with loop B via a bridging water molecule. $2F^{obs}$-F^{calc} map (blue) at 1σ and F^{obs}-F^{calc} map (green) at 3σ (calculated without the water molecule). D) The conformation of loop B remains static also when the phosphomimicking mutation at S115E (blue) is introduced.

3.2.3 CATIONS (PAPER III)

3.2.3.1 Cadmium and calcium

Plant aquaporins can be regulated by cations, most significantly Ca^{2+}, which was first shown in *A. thaliana* suspension cells [81]. From these investigations, it was not clear whether Ca^{2+} is gating the water channels directly, or acting via a signalling pathway. In the first SoPIP2;1 structure [36], it could be seen that a Cd^{2+} ion was situated in a Ca^{2+} binding structural motif at the N-terminus. This motif coordinates a hydrogen bond network connecting loop D to the N-terminus via loop B (Figure 8B). Around the same time, it was shown that Ca^{2+} gated the aquaporin directly on the cytoplasmic side [80]. In the structure, Glu 31 and Asp 28 are

directly coordinating the metal ion, and it was shown by Verdoucq *et al* that mutating these residues decreased the inhibition, particularly for Glu 31 [82]. Also consistent with the structure, the same study showed that mutating the arginine residue connecting loop D to the N-terminus abolishes cation-dependence. This suggests that in the absence of Cd^{2+}/Ca^{2+}, although the binding site might very well be intact, the anchoring point is lost and the channel cannot close. Verdoucq *et al* further showed that Cd^{2+} is a more potent inhibitor than Ca^{2+}. This could explain why cadmium seems to be more successful in locking down loop D for crystallization purposes as we have not yet obtained crystals with calcium as an additive.

In our structure in Paper III, a second metal binding site was identified (Figure 11A). Adding together the presence of Cd^{2+} in the crystallization condition, the strength of the anomalous density when compared to the known Cd ion at the N-terminus and the octaedric coordination, Cd^{2+} is the most probable identity of this ion. This binding site is coordinated by the carbonyl oxygen of Ala 267 (N-terminus), and the side chain of Thr 183 (loop D). Via four coordinating water molecules, further interactions are seen to other side chains and main chain atoms in the C-terminus and loop D. In the first high resolution structure of SoPIP2;1, that of the closed conformation at pH8, a Cd^{2+} ion was not modelled at this location. However, when re-examining the anomalous density map, it is obvious that it does exist with at least partial occupancy. It is possible that also this metal binding site harbours a Ca^{2+} binding site *in vivo*. Interestingly, Alleva *et al* [80] found a biphasic dose-response curve for Ca^{2+} inhibition in *Beta vulgaris* storage roots, leading to the suggestion that there is one high affinity binding site in the nM range, and a second weaker site in the μM range, the latter one possibly corresponding to the site now identified in SoPIP2;1.

Amongst the available SoPIP2;1 structures (Table 2), only those of the wild-type protein with Cd^{2+} bound has a C-terminus which is ordered beyond amino acid 268. The biological role of this second Ca^{2+} binding site could be to help stabilising the C-terminus, favouring the closed conformation through the interactions between Ser 274 and the neighbouring protomer. In this context, it should be mentioned that the C-terminus of the S274E structure is disordered despite the fact that the crystallization condition contains $CdCl_2$. As discussed previously, this can be explained by the phosphomimicking mutation which hinders the interaction between Ser 274 and the neighbouring protomer thereby causing the C-terminus to become disordered.

3.2.3.2 Mercury (Paper III)

Mercury is extensively used as a blocker to prove aquaporin mediated water transport in all types of organisms, and this was a key experiment when searching for, and finally identifying, the putative water channels [7, 10]. If the observed effect on water transport is reversible by a reducing agent, it is considered as proof of a specific oxidation reaction and not a feature caused by mercury's general cytotoxicity. Mercury strongly interacts with the thiol-groups of cysteines, and these residues are normally the cause of mercury-induced inhibition. Still, there is no common mechanism to explain this behaviour or why some aquaporins are completely insensitive.

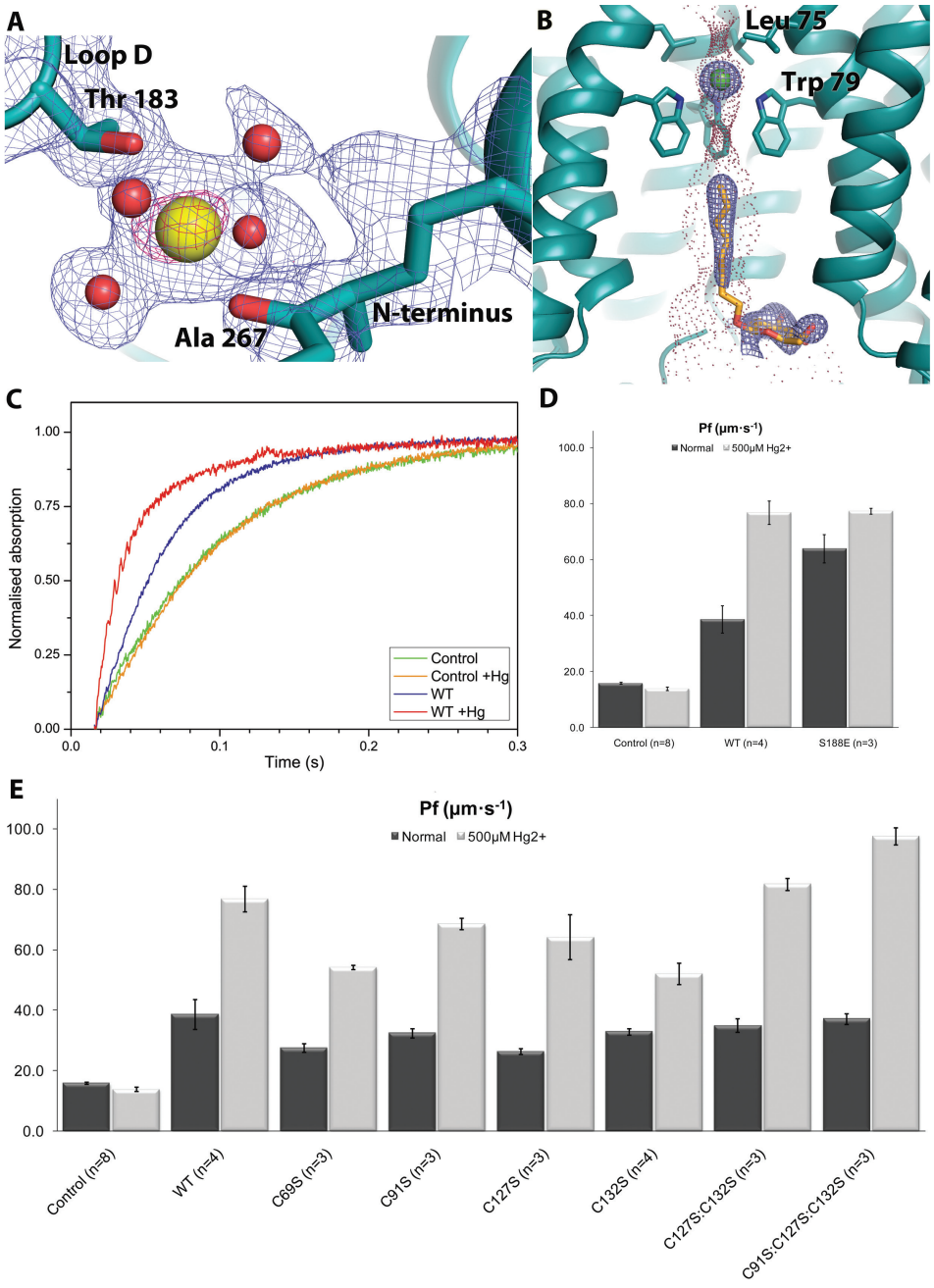

Figure 11. Figures relating to Paper III. A) The new Cd^{2+} binding site. $2F^{obs}$-F^{calc} map at 1σ (blue) and anomalous map at 3.5σ (pink). B) The middle pore showing density for the β-OG molecule (orange) and the Cl^- ion (green). The pore profile is shown as purple dots. C) Stopped-flow curves for SoPIP2;1 with and without mercury. D) Comparison of water transport rate (P_f) for SoPIP2;1 wild-type and the S188E mutant. E) Comparison in water transport rate (P_f) for SoPIP2;1 wild-type and cysteine-to-serine mutants.

In one case only, hAQP6, activation by mercury has been described [100]. Thus, it was much to our surprise that we noted an increase in water transport for mercury-treated SoPIP2;1 in proteoliposomes (Figure 11C). Given our interest in the gating mechanism of plant aquaporins, we hoped that further studies of this subject would provide insights into activation of the channel. Thus, the structure of mercury containing SoPIP2;1 was solved and cysteine-to-serine mutants were investigated in proteoliposomes water transport assays. Mercury was clearly seen to bind to three out of four cysteines in the structure; Cys 91 in the end of TM2 as well as Cys 127 and Cys 132 in the middle of TM3 (Figure 7). The fourth cysteine, Cys 69, is not available as it is forming a disulphide bridge to the same residue in a neighbouring protomer. However, mercury binding caused no structural perturbations beyond the binding site and the pore remained occluded. In addition, the water transport ability of any of the cysteine mutants did not differ significantly from the wild-type (Figure 11E). Hence, no single cysteine could be identified as responsible for the activating effect.

When comparing the SoPIP2;1 data to what is known about mercury interaction with other aquaporins, no clear patterns can be seen. For several mammalian aquaporins, the inhibitory effect is connected to a cysteine in the constriction region that lines the water conducting pore (Figure 3). Structural studies of the bacterial AqpZ that was mutated to imitate human AQP1 showed that when mercury binds at this site, the pore is sterically occluded [41]. Molecular dynamics simulations also indicated that mercury binding causes a collapse of the ar/R region [101]. The cysteine identified as being sensitive to mercury in AQP1 is not well conserved outside of the mammalian aquaporins, and in particular not among plant aquaporins. Still, in plant research, inhibition by mercury is extensively used to confirm the role of aquaporins in water transport [98, 102, 103]. Site-directed mutagenesis has pinpointed a cysteine residue in TM3 to be responsible for mercury inhibition in two TIP aquaporins in *A. thaliana* [104]. These two TIP:s lack the cysteines of SoPIP2;1, but in a sequence alignment the identified cysteines are only two residues away from Cys 132. However, this feature is not conserved among many aquaporin variants displaying mercury sensitivity [105-107], and is still present for one insensitive isoform [105]. Of 15 PIP:s with exactly the same pattern of cysteines as SoPIP2;1, four are insensitive to mercury [106, 108, 109] while the rest are inhibited [105-107, 110]. For the legume *Medicago truncatula* aquaporin MtAQP1, a slight increase of water permeability was reported upon mercury treatment in the oocyte system [111], but this aquaporin does not contain any cysteines at all. Taken together with our results, the conclusion must be that mercury sensitivity by aquaporins cannot be explained solely by interaction with cysteines.

Since we use purified protein in proteoliposomes, indirect effects mediated by other proteins can be ruled out. What remains is the lipids constituting the liposomes. NMR measurements have revealed that there is a significant interaction between mercury and phospholipids containing primary amines, in particular phosphatidylethanolamine [112]. This lipid is the major constituent of *E. Coli* polar lipid extract used to form liposomes. Mercury lowers the membrane fluidity causing the water to diffuse slower through the stiffer membrane [113] and in line with this argument, our control liposomes are slightly reduced in water transport rate when mercury treated. Membrane proteins are an integrated part of the bilayer and the

mechanical properties of the membrane can affect protein conformation and the equilibrium between different conformational states [114, 115]. Mechanosensitive gating has been implicated for aquaporins before, both for AQP4 [114] and *P. pastoris* AQY1 [38]. The increase in membrane stiffness after mercury treatment could have small effects on the conformation of the transmembrane helices in SoPIP2;1, affecting the channel so that water can pass faster. *In vivo*, the same effect could be achieved by changing the membrane composition with respect to e.g. cholesterol.

3.2.4 GATING IN THE PLANT – THE INTEGRATED EFFECT OF SIGNALS

Cells receive a flood of information concerning the state of the environment, and at every moment in time the location and activity of the aquaporins must match the need for water intake, and in some cases possibly gases and ions (see section 3.2.6.1). Drought, flooding, chilling and salt stress are some factors that have been shown to affect aquaporin activity in plants [69]. In addition to direct gating, this happens through changes in cellular trafficking and gene expression. The delicate balance of all these factors determine the outcome, and the full picture of how this is achieved is still not clear. In most studies, different factors are investigated individually, and it is difficult to predict what will happen in the real plant when many and sometimes contradicting signals is at work at the same time.

From the structure, the completely conserved Ser 115 seems to be the more important phosphorylation site, since its phosphorylation directly destroys the calcium binding site and prevent loop D from closing. The relevance of Ser 274 is more not to be in the way, when some other signal tells the channel to open. Thus, although phosphorylation at this site does not provoke pore opening in its own right, the status affects the equilibrium between the open and closed conformations. The respective roles of the phosphorylation sites are supported by functional assays which have shown a dramatic effect for Ser 115, while data is less clear for Ser 274. The caveat is that only Ser 274 has been unambiguously shown to be phosphorylated *in planta*.

Dephosphorylation is thought to be connected to drought stress, during which circumstances it is important for the plant not to lose excessive amounts of water [83]. The opposite of drought is flooding, which causes anoxia in the cell. This is connected to a decrease in pH [96] and in addition, Ca^{2+} levels may also increase [116]. Both factors will favour the closed conformation of PIP:s. The low pH structure shows how the channel can be kept closed even if no Ca^{2+} is present at the metal binding site. Surprisingly, mutating the correspondent to the pH probe His193 in AtPIP2;1 had a dramatic effect also on cation sensitivity, indicating a previously undescribed interplay between the regulation mechanisms [82].

To conclude, in a state of high Ca^{2+}- concentration, low pH and little kinase activity, all known factors cooperate to close a PIP aquaporin channel. However, most of the time the signalling pattern is not so clear and an individual channel is likely fluctuating between its closed and open conformation. Thus, it is not a simple "on and off" system, but rather a carefully regulated equilibrium that is pushed in a certain direction by the current signals.

3.2.4.1 Heavy metals and plants

In this thesis, cadmium and mercury have been used as tools to study the activity of aquaporins. However, pollution by these heavy metals is a serious environmental problem that poisons all types of living organisms. These metals are non-essential but imitate other minerals that are required for many biological processes and are thus taken up in cells. The widespread effects include breakdown of cell structure and organelles like mitochondria and thylakoids, as well as increased generation of reactive oxygen species causing oxidative damage in the plant cell [117, 118]. Few studies have examined the roles of aquaporins in this context, but it is known that the water balance in plants is affected by heavy metals [119]. A study on how several heavy metals affected water transport in onion cells showed that mercury and cadmium were the most potent inhibitors and that this effect is one of the first responses to heavy metal stress [120]. Cd^{2+} has also been shown to be a stronger blocker than Ca^{2+} of individual aquaporins in a purified system, showing a specific effect of this heavy metal that might be problematic for the plant in its natural context [82].

3.2.5 OTHER STRUCTURAL FEATURES OF SOPIP2;1

3.2.5.1 Central pore (Paper III)

A subject of debate for aquaporins is whether the central pore formed by the tetramer can conduct some type of molecules or not. In some structures, membrane lipids have been found in the middle of this channel, clearly prohibiting passage in those cases [35, 40]. Several reports exist where transport of CO_2, NH_3 and NO through aquaporins has been measured [121, 122]. Especially CO_2 transport in red blood cells and plants has attracted attention due to its relevance for respiration and photosynthesis [121, 123]. However, the results have been heavily questioned as there is a long standing view that it is not the transport through membranes that is the limiting factor for CO_2 transport, but rather the crossing of an unstirred water layer close to the membrane. There are also some technical difficulties which make experimental results difficult to interpret [121, 124, 125]. Nevertheless, experiments indicate that CO_2 is indeed transported through some plant aquaporins. A PIP1 aquaporin in tobacco seems to increase CO_2 transport in chloroplasts [126] and experiments in yeast showed that this transport is cooperative, indicating transport through the central pore rather than the individual water channels [78]. No CO_2 transport could be detected for a PIP2 homolog, and likewise a knock-out of *A. thaliana* PIP1;2 decreased the CO_2 transport in mesophyll cells whereas deletion of AtPIP2;3 had no effect.

Structural studies of the central pore are often hampered by the inherent tendency of aquaporins to crystallize so that the central pore of the tetramer coincides with a crystallographic fourfold symmetry axis, which makes the electron density here difficult to interpret. In the high resolution structure with mercury this is avoided due to a primitive orthogonal space group. Two density features are seen in this location (Figure 11B). The first is a continuous stretch of elongated electron density with a bulkier head group that can be seen at the intracellular side of the central pore in both tetramers. As mentioned above, lipids have been modelled at this position in other aquaporins, but in this case, the length corresponds to only six carbons, which is not likely to correspond to any membrane lipid.

However, this agrees well with a β-OG molecule, which is the detergent used in the purification process. The second feature is a very strong (21σ) but non-anomalous spherical difference density is seen 8Å further up in the pore, coordinated by the indole ring nitrogens of four tryptophan residues (Trp 79), one from each protomer. Tryptophans are virtually never seen coordinating metal ions [127], but can act as hydrogen bond donors. When modelling this density as Cl^-, no difference density remains and the B-factors agree well with the surrounding tryptophans and the bond lengths (~3.2Å) is similar to what has been observed for tryptophans hydrogen bonds before [128]. Since NaCl is present during purification and crystallization, Cl^- seems to be a probable choice at this site. The question remains as to how the ion got there, or if it could escape again. A calculation of the pore diameter shows that the putative Cl^- ion is surrounded by a narrow, hydrophobic waist on each side, created by the rings of four Leu 75 and Trp 79, with a radius of 0.55Å and 0.61Å respectively (Figure 11B). The ionic radius of Cl^- is considerably larger; 1.7Å, and this part of the protein has low B-factors, indicating low flexibility in the crystal. If some aquaporins are transporting substances in the central pore, there must be sufficient room here for these molecules to pass. Judging from the amino acid sequence, the motif at the narrow passage is preserved in both the CO_2 transporting PIP1:s, although the leucine is exchanged for a isoleucine, possibly widening one of the waists somewhat.

There are some reports of ion transport in aquaporins [129], but the molecular mechanisms are unclear and seem to differ between isoforms. AQP1 has been suggested to conduct cations through the central channel [129], and the plant NIP aquaporin Nodulin 26 showed conductance of both cations and anions that could be gated by phosphorylation by the correspondent to Ser 274 [130, 131]. In one other case, the bacterial glycerol transporter GlpF, the presence of ions in the central channel has been reported [14]. In this case, two Mg^{2+} ions separated by water were modelled. One of these ions was coordinated by four tryptophans in a similar way as the Cl^- ion in SoPIP2;1 mentioned above. However, in this case the central pore is on a fourfold crystallographic axis so the interpretation is difficult. Moreover, in the deposited PDB coordinates, the ions were replaced by 3 water molecules at 25% occupancy. Thus, the identity of this density remains unclear.

3.2.5.2 Why closed structures?

Following the initial SoPIP2;1 structures, much effort has been devoted to determining a better resolution structure of the open conformation. However, this has not yet succeeded (Table 2). Experience from crystallization trials shows that whenever Cd^{2+} is added, any formed crystals will be closed, even if the channel has been mutated to mimic the open state (S274E) [37], or if the pH favours an open channel [36]. The closed structure represents a compact, stable form of the protein and is hence favoured by crystallization. It is likely that the protein is flexible between opening and closing states when not incorporated in a crystal, as we do detect fast water transport in proteoliposomes (). But since this is a matter of equilibria, the initial crystal nucleus formed is more likely to contain protein molecules that happen to be in the closed conformation, and further closed molecules fitting into this packing pattern are then recruited. When the likelihood of an open channel is very high, as

for the S188E mutant, the resolution of the formed crystals is drastically reduced (unpublished observations), indicating weaker crystal packing interactions.

When inspecting the packing of SoPIP2;1 crystals (Figure 12), it is obvious that this molecule often packs with the intracellular regions facing each other with little space left for loop D to swing open. This is seen for 1Z98 (wt closed), 3CN6 (S274E) and 4JC6 (Mercury) (Figure 12A-B). In 2B5F (wt open) and 41A4 (low pH), there is more space, but the price for this looser packing is a decrease in resolution (Figure 12C). Only in this packing, an open conformation has been observed. The packing in 3CLL (S115E) and 3CN5 (S115ES274E) is more dense (Figure 12C), but there seem to be space for an open loop as the intracellular sides are not in direct contact. Still, the structures remains closed. As previously discussed, this is most likely due to serine-to-glutamate mutation not fully mimicking the phosphorylated state although the cadmium binding site is disrupted.

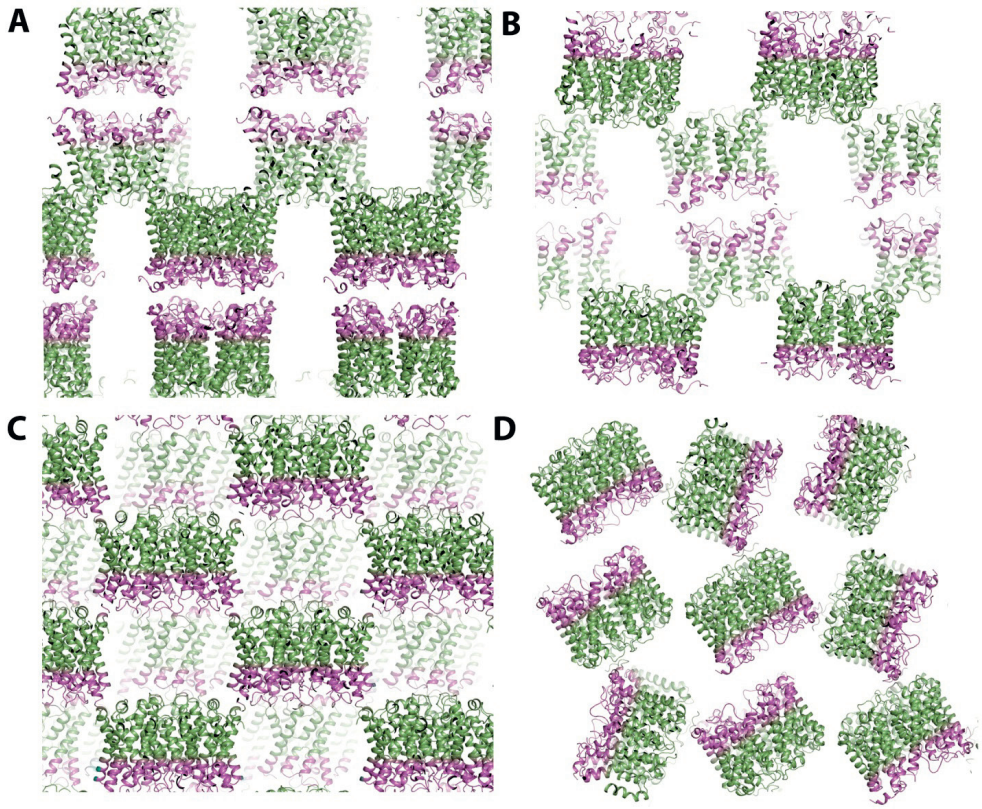

Figure 12. Packing of SoPIP2;1 in different crystal forms. A: 1Z98 and 3CN6, B: 4JC6, C: 3CLL and 3CN6, D: 2B5F and 4A14. The intracellular part containing loop D has been coloured in violet.

Table 2. Structures of SoPIP2;1. If protomers are resolved to different extent, the amino acid range for the longest protomer is stated.

Protein (PDB-code)	Wt closed (1Z98)	Wt open (2BF5)	S115E (3CLL)	S115ES274E (3CN5)	S274E (3CN6)	Low pH (41A4)	Mercury (4JC6)
Resolved amino acids	24-274	28-263	27-267	32-268	24-266	20-267	23-274
Extracellular side exposed?	No	Yes	Yes	Yes	No	Yes	No
Reference	[36]	[36]	[37]	[37]	[37]	Paper II	Paper III
Crystallization condition	30% PEG400 0.1M Tris pH 8 0.1M NaCl 0.1M $CdCl_2$ as additive	30% PEG400 0.1M sodium citrate pH 5.6 0.1M NaCl	32% PEG400 0.1M MES pH 6.5 0.1M NaCl	30% PEG 400 0.1M MES pH 6.5 0.1M NaCl 0.1M $MgCl_2$	24% PEG400 0.1M Tris pH 7 0.2M NaCl 0.1M $CdCl_2$ as additive	22% PEG400 0.1M sodium citrate pH 6 50mM NaCl 20mM $MgCl_2$ Protein $HgCl_2$ incubated	26% PEG400 25mM Tris pH 7.0 0.1M NaCl 0.1M $CdCl_2$ as additive. Protein $HgCl_2$ incubated
Conformation	Closed, 2 protomers	Open (1/4 protomers)	Closed, 1 protomer	Closed, 1 protomer	Closed, 2 protomers	Closed, 4 protomers	Closed, 8 protomers
Space group	I4	$P2_12_12$	I4	I4	I4	$P2_12_12$	$P2_12_12_1$
Resolution	2.1 Å	3.9 Å	2.3 Å	2.05 Å	2.95 Å	3.1 Å	2.15 Å

4 Human aquaporins

In humans, 13 aquaporin homologues have been found. They are distributed throughout the body, and affect many aspects of our biology (Table 3). The sequence similarity for some isoforms is very high, with the maximum being 62% identity between AQP2 and AQP5 (Figure 13). At the other end of the spectra, AQP2 and AQP11 are the most dissimilar, sharing only 13% of their amino acid sequence.

Table 3. Basic facts about the human aquaporins. Information from [132] and [133] unless otherwise indicated. Disease states identified in patients are written in italic.

Protein	Selectivity	Examples of tissue distribution	Implications in disease, (examples)
AQP0	Water	eye lens,	*Cataracts*
AQP1	Water	red blood cells, kidney, lung, brain, eye	*Mild urinary concentrating deficiency*, tumour angiogenesis
AQP2	Water	kidney, inner ear, male reproductive organs [134]	*Nephrogenic diabetes insipidus*
AQP3	water, glycerol, urea	skin, kidney, airways, eye	Skin hydration and elasticity, wound healing
AQP4	Water	brain, kidney, eye, airways	Brain edema
AQP5	Water	pancreas, salivary gland, lacrimal gland, sweat gland, lung, eye	*Sjögren's syndrome*
AQP6	water, anions	kidney	
AQP7	water, glycerol, urea, arsenite	adipose tissue, kidney	Obesity
AQP8	Water	kidney, liver, pancreas, small intestine, testis, colon	
AQP9	glycerol, urea, small solutes, arsenite, water	liver, brain	
AQP10	water, glycerol, urea	small intestine[135]	
AQP11	Unclear	kidney	
AQP12	Unclear	pancreas [136]	

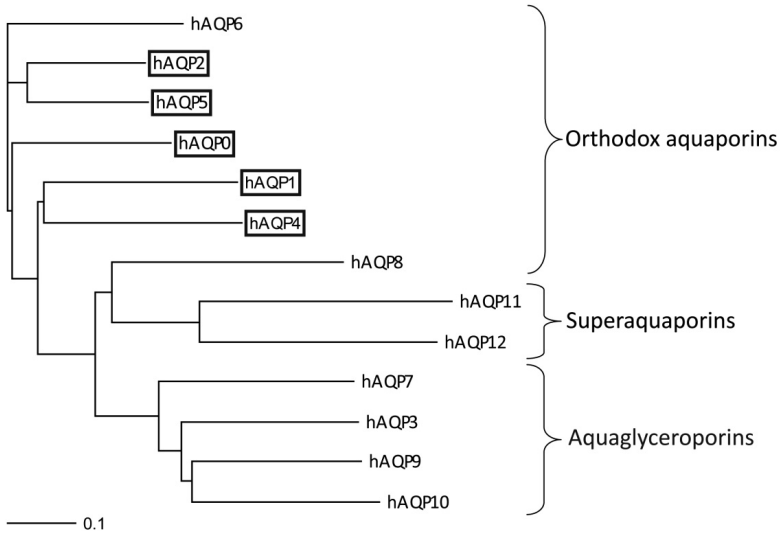

Figure 13. Phylogenetic tree of the human aquaporins. For isoforms marked with a box, a structure is solved for some mammalian species.

4.1 AQUAPORIN 2

4.1.1 THE ROLE OF AQUAPORIN 2

The aquaporin 2 gene was first cloned from mRNA found in rat kidney [137]. In the kidney, AQP2 is present in the collecting duct principal cells. It has also been found in the inner ear and in male reproductive organs. The exact role in the latter tissues has not yet been established [134], but in the kidney, AQP2 is a crucial player in maintaining water homeostasis.

The kidney is the key organ for water balance within the body. 180 litres of primary urine is filtrated here every day in an adult man. Blood plasma is filtered in the renal corpuscule (Figure 14A), and is then passed through the winding tubing system of the nephron. Several nephrons empty in a common collecting duct and before the urine is emptied into the ureter, around 99% of the water has been reabsorbed into the body. Several aquaporin homologues participate in this process [138]. AQP1, and to a lesser extent AQP7, take back 90% in the proximal tubules in an unregulated fashion. The remaining part is taken care of by AQP2 in the collecting duct (Figure 14B), where it is responsible for the fine adjustment necessary to meet the present needs of the individual [139, 140]. Thus, it is necessary to have exact means to regulate this aquaporin. Contrary to plant aquaporins, this is not mediated by direct gating. Instead, this is achieved by adjusting the amount of aquaporin present in the membrane, a process referred to as trafficking, and it is as a model protein in this context that AQP2 has received much attention. In addition, AQP2 was one of the first aquaporins to be directly linked to disease states, most notably the water balance disorder nephrogenic diabetes insipidus (NDI).

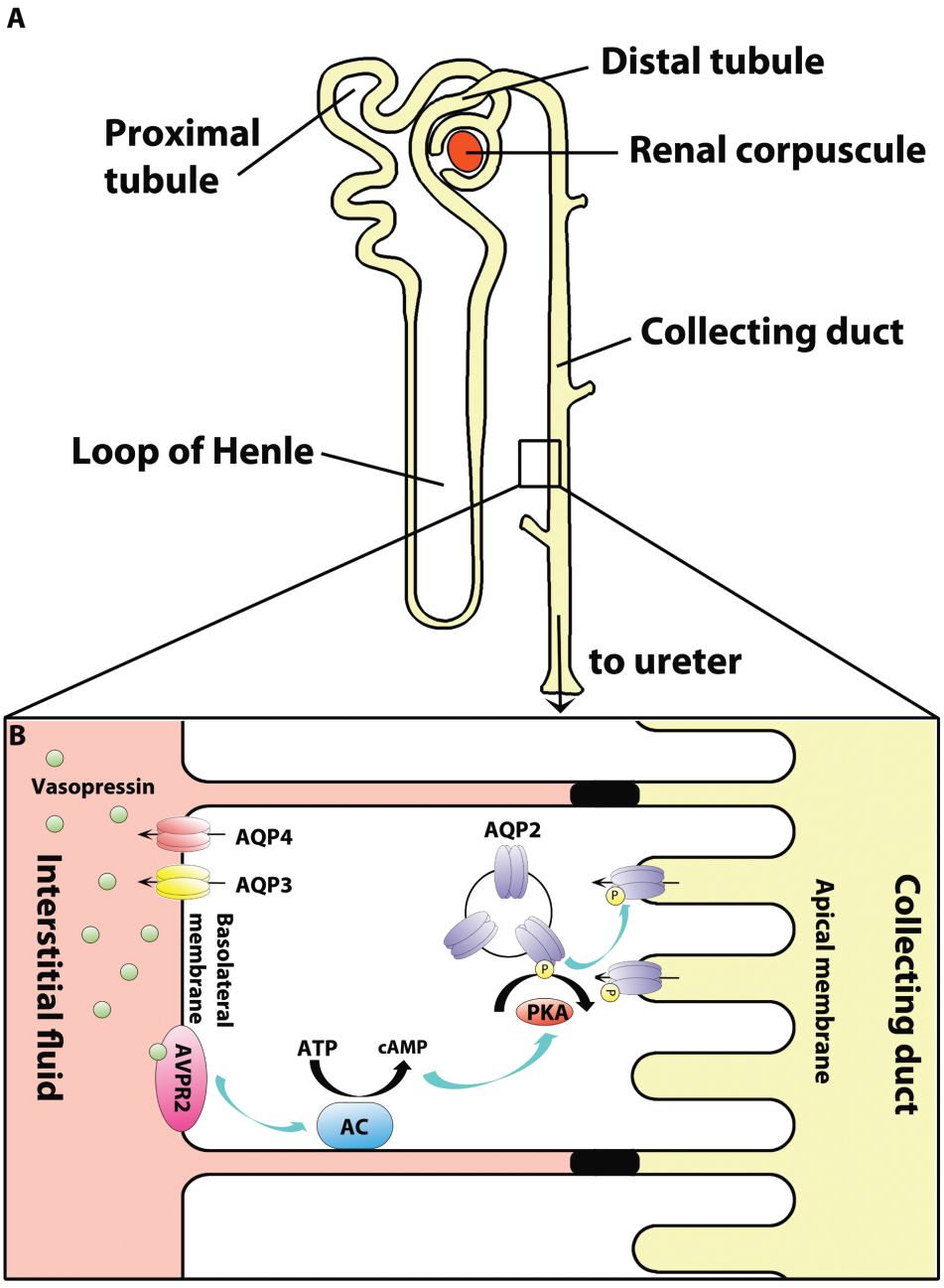

Figure 14. A) The blood is filtrated in the renal corpuscule and the primary urine is passed through parts of the nephron until it reaches the collecting duct where AQP2 is situated. B) Regulation of AQP2 in the principal cells. Binding of vasopressin starts a signalling cascade involving the V2 receptor (AVPR2), adenylate cyclase (AC) and protein kinase A (PKA).

AQP2 shares its basic topology with all other aquaporins (Figure 15, section 1.2.2). Distinguishing features include a relatively short N-terminus and an extended C-terminus. In addition to this, several sites are subject to posttranslational modifications.

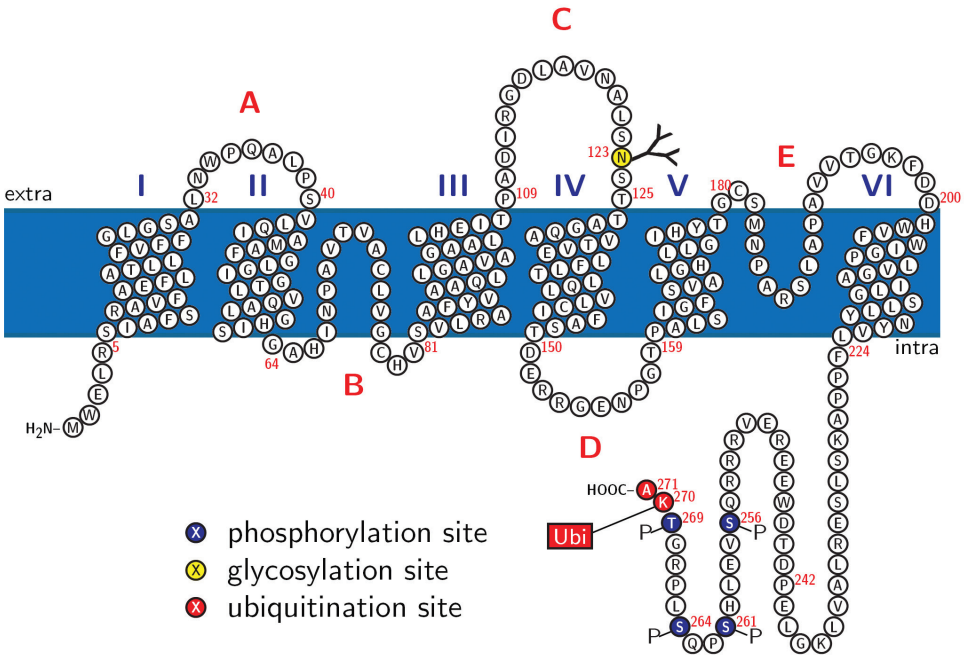

Figure 15. Topology of AQP2 with some sites for posttranslational modifications marked.

4.1.1.1 Trafficking

The idea that the water channel responsible for urine reabsorption is shuttled between the plasma membrane and an intracellular compartment in response to vasopressin had been launched already in 1975 [8]. These experiments were in themselves arguments in favour of the existence of the yet unidentified aquaporins. 20 years later, the role of AQP2 in vasopressin mediated water flow was finally confirmed [139]. Vasopressin is a hormone released from the posterior pituitary gland which binds to the V2 receptor (AVPR2), a G-coupled protein receptor. This starts a signalling cascade (Figure 14B) involving the generation of cAMP, activation of Protein Kinase A (PKA) and eventually phosphorylation of AQP2, which results in trafficking to the apical plasma membrane. Once incorporated, AQP2 starts to transport water into the cell, which is then transported further into the body by AQP3 and AQP4 in the basolateral membrane. Exactly how the phosphorylation by PKA induces trafficking to the plasma membrane is still an open question. It is established that phosphorylation of several residues in the C-terminal domain of AQP2 are involved (Figure 15), with Ser 256 being the most prominent site, aided by Ser 269. The role of Ser 261 and Ser 264 is more unclear [141]. The phosphorylation level of AQP2 once it is incorporated into the plasma membrane governs the internalization rate [142] and delaying this process is just as important as the original targeting to increase water transport. Internalization and

eventual degradation as a result of ubiquitination at Lys 270 [143] is also a factor, and both types of post-translational modifications might cooperate.

Vasopressin is an AQP2 regulator on several levels. In the short term, vasopressin stimulates trafficking as described above which gives elevated levels of AQP2 in the apical membrane within 5-30 min [138]. If the vasopressin concentration is remains high for at least 24h, long-term regulation is also seen through increasing AQP2 transcription [138, 144].

On its route to and from the plasma membrane, AQP2 must be helped by other proteins which ensure its proper targeting, based on the posttranslational modifications displayed. Studies show that this involve cytoskeletal proteins like microtubulin [145], myosin [146] and direct interaction with actin and tropomyosin [147]. Internalization is thought to be mediated via clathrin-coated pits and the known clathrin uncoating protein heat-shock protein70 has been recognized as a direct interaction partner [148]. Furthermore, LIP5, a protein participating in the sorting of proteins for lysosomal degradation, interacts with the proximal part of the C-terminus of AQP2 [149].

4.1.1.2 Pathology

Defects somewhere in the signalling pathway that induces trafficking of AQP2 to the plasma membrane result in impaired urine concentrating ability. In most cases, this is an acquired disease, often a side-effect from lithium treatment of bipolar disorders [144]. However, in 10% of the cases, the disease is inherited, and the causing mutation can be in either the AVPR2 receptor or in the AQP2 gene. The resulting disease, nephrogenic diabetes insipidus (NDI), manifests itself by very large urine volumes and, as a consequence, severe dehydration. If not properly treated, the result is a substantial weight loss and high risk of mental retardation due to several incidents of fast changes between brain dehydration and edema when cycling between de- and rehydration. Urine concentrating problems is diagnosed as diabetes insipidus if the urine volume is exceeding 3L/24 hours for an adult [150], but 10-15L is described in some cases [151, 152].

Mutations in the AQP2 gene can be of either a dominant or recessive phenotype, with the latter being the more common (90% of cases). In the recessive form, the effect of a majority of the mutations is that the protein is retained in the ER as the cell perceives the protein as misfolded. Thus, when vasopressin signals the need for water absorption, no AQP2 is available for trafficking [144, 150]. However, it has been shown that some AQP2 mutants are actually functional water channels even though they are trapped in the ER, indicating that the degree of misfolding is not necessarily very large [150]. In the dominant form, the mutation is located in the C-terminal part of AQP2 and interferes with signalling mechanisms. Due to its heterooligomerization with normal AQP2 molecules originating from the healthy chromosome, the entire tetramer is misrouted or degraded. Luckily, some tetramers still manage to function properly, which makes the dominant form of the disease less severe than the recessive [150].

Syndromes coupled to water retention such as congestive heart failure and preeclampsia (toxicity of pregnancy) can also be coupled to increased display of AQP2 in the plasma

membrane. The problem is then normally connected to elevated vasopressin levels that induce too extensive plasma membrane localization [138, 144].

4.1.2 FROM GENE TO CRYSTAL – OPTIMIZATION OF PROCEDURE

An electron crystallographic structure of human aquaporin 2 (hAQP2) exists which is derived from protein produced in insect cells [153]. However, the resolution is limited to 4.5Å in the membrane plane and 6.7Å in the perpendicular angle. Thus, the position of transmembrane helices can be modelled, but the main chain cannot be traced. In addition to this, there is some residual density below the protomers that was speculated to be the N- and C-termini. In order to understand AQP2 and how it differs from the other aquaporins harboured in our bodies, better structural data was needed. We can now present X-ray crystallographic structure of hAQP2 to 2.95Å, but the process of obtaining this was not straight-forward. Hence, this experimental process will be discussed further here.

4.1.2.1 Optimization of construct and production

When it was decided to undertake the task of solving the structure of hAQP2 in our laboratory, two production hosts were investigated. One of these was *Pichia pastoris*, but the low production level stopped these attempts at an early stage. A comparison of the production level of all aquaporins showed that AQP2 was one of the proteins giving the lowest yield, despite its similarity to the well producing AQP5 [154]. Instead, a lot of effort was invested using AQP2 produced in Sf9 insect cells. Diffraction spots at 3.7Å were seen at best, but these crystals were anisotropic, poorly reproducible and did not freeze well as they grew in PEG1000 and were difficult to cryoprotect (Figure 16A-C). Furthermore, it was clear from SDS-PAGE that the samples were not homogenous as several bands were visible below the monomer (Figure 16D-E).

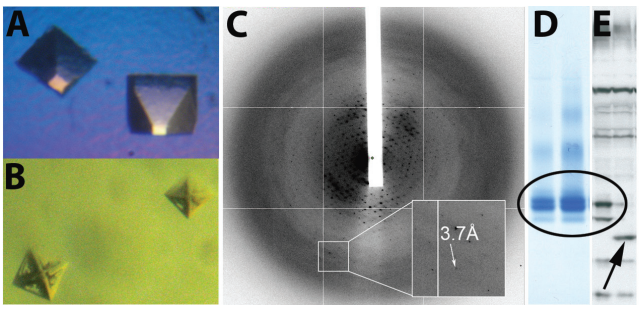

Figure 16. Results from initial attempts to purify and crystallize aquaporin 2. A) Examples of good crystals from the insect material and B) more representative ones with visible defects. C) The best diffraction observed for AQP2 produced in insect cells. D-E) SDS-PAGE of AQP2 produced in insect (D) and yeast (E). Attempts to produce full length constructs resulted in inhomogenous protein (black circle) with three visible bands for the insect material and two in yeast. When the C-terminus was removed, only a single band for the monomer was seen (arrow).

This led us to reinvestigate the *Pichia pastoris* strategy since both the genetic work and the production procedure is much simplified and this was an in-house technology. The cause of the inhomogenity was investigated with selective staining and mass spectrometry, but no

differences in either length, phosphorylation or glycosylation could be detected. However, if the C-terminus was removed, only one band was seen (Figure 16E). A comparison of determined structures of aquaporins (Figure 17) shows that in no case has the C-terminus been resolved further than in AQP5. For AQP5, there are strong indications that the best crystals came from a batch of protein that to a large extent was endogenously degraded in the C-terminus. When analyzed on SDS-PAGE, the best crystals were shown to be built up by this truncated form [Rob Horsefield, personal communication]. Moreover, it was crucial to trypsinate the protein to achieve well diffracting crystals of AQP4 [32]. Hence, there were strong indications that it would be beneficial for crystallization to remove part of the C-terminus, a part that would most likely not be resolved in the structure anyway.

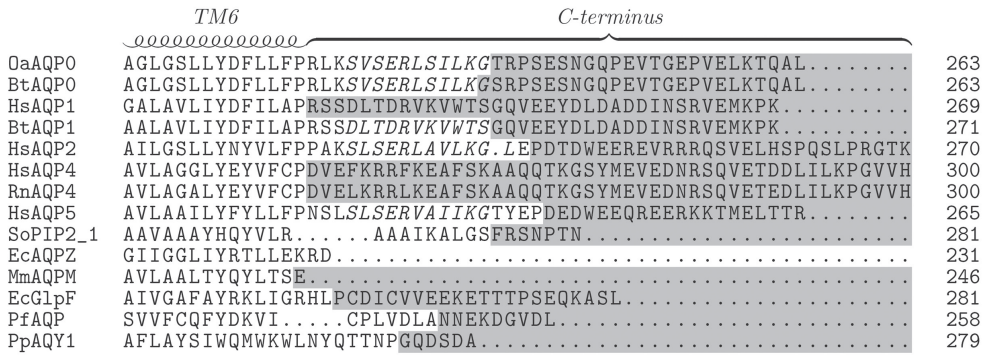

Figure 17. Alignment of the C-terminus of structurally determined AQP:s. Unresolved parts of the C-terminus are shaded in grey. Residues forming a C-terminal helix in solved structures are marked in italic. The last 23 amino acids of AQP4 have been omitted.

In total, over 30 AQP2 constructs for *Pichia pastoris* were cloned and evaluated for production. The gene sequence was codon optimized, the effect of removing posttranslational modifications was investigated, and different lengths of the C-terminus was evaluated. The effect of the size and position of the his-tag as well as the type of protease site that separated the tag and the protein was also looked into. When evaluating these factors, two clear trends could be noted; the his-tag should be placed in the N-terminus, and truncated version of the protein express better than the full length construct. The best performance was seen for a construct, "FOB2" that was truncated at Pro 242 (corresponding to the last visible residue in AQP5) with an N-terminal his-tag connected to the protein via a TEV protease site (Figure 18A). Curiously, this construct contained a W2S mutation resulting from the delivered PCR primer being faulty. It would be interesting to check if this mutation is related to the increased production. The FOB2 construct, and a similar construct that was extended to His 260 with a phosphomimicking S256E mutation, was taken further to purification, but the first one proved to be more stable and hence the efforts were focused here.

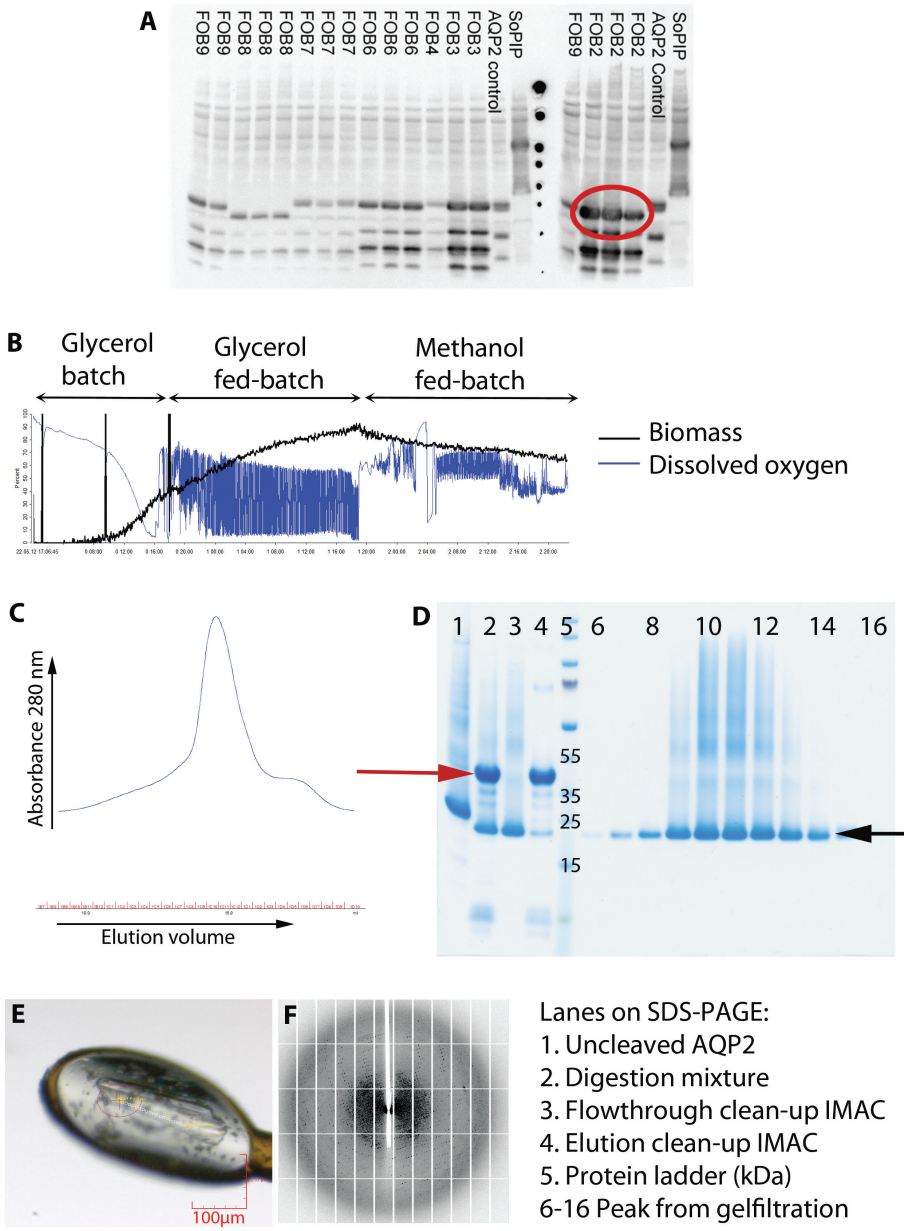

Figure 18. From production to diffraction for AQP2. A) The construct "FOB2" (red circle) was superior in production level when compared to a range of other constructs. B) Fermentation of AQP2. A "spiking" dissolved oxygen-signal indicates that the cells metabolize the fed carbon source immediately. Towards the end of the fermentation, this behaviour decreases. C) Chromatogram from gel filtration of AQP2 in OGNPG. D) SDS-PAGE showing the performance of TEV protease digestion and gel filtration. Black arrow indicates the AQP2 monomer. E) The best AQP2 crystal mounted in a loop at the synchrotron. F) Diffraction to below 3Å from the crystal in E).

Some investigations of the optimal production protocol have been done, but neither lowering the temperature nor providing a mixed feed with methanol and sorbitol improved the production. A fermenter culture grown at lower OD than normally did not perform better either. Around 24h post induction, the cells gradually stop responding to methanol, and pursuing beyond this point is not beneficial for the production level (Figure 18B).

Table 4. Crystal forms for hAQP2. Resolution is for scaled data.

Space group	I4	I4	$P2_12_12_1$	C222	P42
Cell dimensions	94*94*169Å α=β=γ=90°	92*92*171Å α=β=γ=90°	95*108*133Å α=β=γ=90°	94*94*166Å α=β=γ=90°	119*119*91Å α=β=γ=90°
Resolution	3.8Å	4.8 Å	4.8Å	4.7Å	2.95Å
Twinning	50%	Unknown	No	Unknown	No
Detergent	NG	β-OG	NG	NG	OGNPG
His-tag	Uncleaved	Uncleaved	Cleaved	Cleaved	Cleaved
Crystallization condition	24%PEG400 0.2M citrat 0.1M Tris pH9. Additive: 0.15mM Cymal7	20%PEG400 Tris pH9 0.1M MgCl2	20%PEG400 0.1M Tris pH9 0.1M NaCl 0.1M MgCl2	26%PEG350 MME 0.04M Tris pH9 0.04M NaCl	22%PEG400 0.1M Tris pH8.5 0.1M NaCl 0.1M $MgCl_2$ Additive: 0.1M $CdCl_2$
Morphology	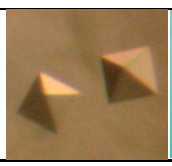	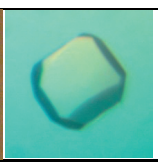	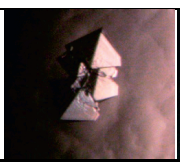	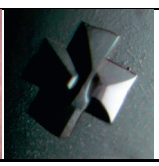	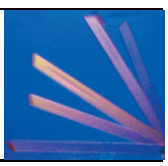

4.1.2.2 Purification and crystallization procedure

Nonyl glucoside was chosen as solubilization agent which together with 8 histidines in the affinity tag ensured an efficient IMAC purification step. The peak from gel filtration was homogenous in shape and contained pure protein (Figure 18C-D). AQP2 easily crystallizes and crystallization screens frequently give beautiful small pyramids in many conditions. Unfortunately, these crystals seldom diffract well and a main difficulty in the project has been to determine what conditions that actually improve diffraction results and not only gives crystals that are pretty to look at. In total, over 800 crystals were screened at the synchrotron for the FOB2 construct before the structure was solved, and prior to that, 400 from AQP2 expressed in insect cells. The first condition to give diffraction data which allowed attempts to solve the structure gave crystals in the apparent space group I422 (Table 4). However, this data could not be solved until twinning was taken into account and the results showed that the crystals were perfectly twinned and the real space group was I4. Twinning is a packing

defect in crystals where a fraction of the molecules are packed in a different way compared to the others. When both domains are equally large, this is referred to as perfect twinning. Twinning is problematic for the structure solution process, especially in the perfectly twinned case. Still, this is an issue that sometimes can be handled and this was successfully done for e.g. AQP5 [35]. However the combination of poor resolution and perfect twinning is very difficult and the best solution in these situations is to find another crystal type. This was particularly true in this case, since the resolution would not improve despite extensive efforts. Switching detergent to the shorter β-OG gave crystals of the same type but with a small shift in cell dimensions, consistent with the smaller micelle, but the resolution did not improve (Table 4). When the his-tag was cleaved off, several new crystal types appeared with new interesting morphologies (Table 4). The final breakthrough came when the detergent was exchanged to OGNPG and $CdCl_2$ was added to the crystallization mixture. This combination led to a new type of crystal that gave data to 2.95Å (Figure 18E-F), a resolution that allows the main chain and the majority of the side chains to be modelled.

Exactly why OGNPG was a better choice of detergent is not clear but despite it being a very novel detergent, it has already given new structures of membrane proteins [155]. The role of cadmium is more obvious from the structure where two sites binding this ion can be observed (Figure 20C). What seem to have happened is that the first cadmium ion, Cd1, situated at the interface between protomer A and D, directs the conformation of loop D of protomer A. The result is that a pocket is exposed in protomer D where the C-terminus from another tetramer can bind, a conformation which is further stabilized by the binding of a second cadmium ion, Cd2. This specific interacting gives a much more defined packing pattern than the crystals of the I4 type (Figure 19), thus likely improving the resolution and reducing the risk for misoriented tetramers resulting in twinning.

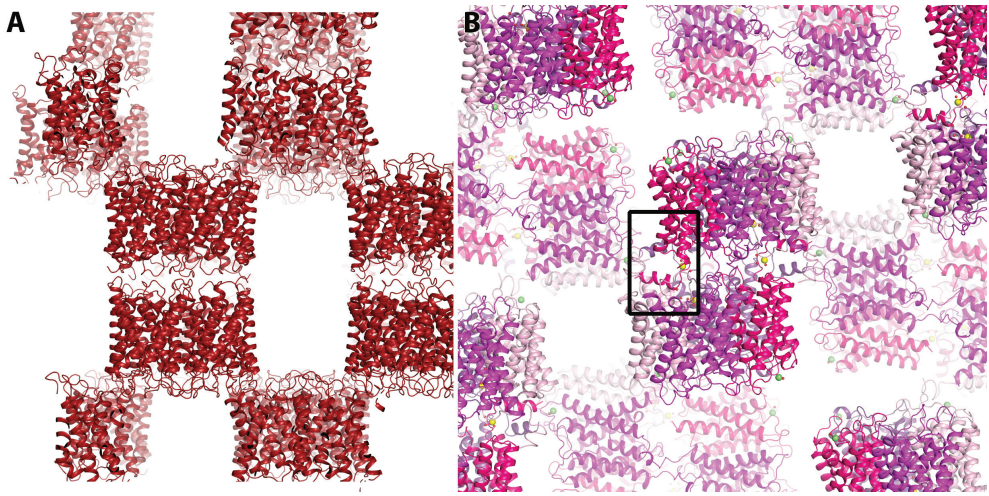

Figure 19. Packing of AQP2 molecules in the A) I4 and B) $P4_2$ crystal form. In $P4_2$, the C-terminal helix of one protomer (pink) interacts with a symmetry related tetramer (black box), hence creating a more defined packing pattern.

4.1.3 STRUCTURE OF AQUAPORIN 2 (PAPER IV)

The asymmetric unit of our AQP2 structure contains one tetramer with clear structural differences between the four protomers. At a resolution at 2.95Å, the main chain can be traced for amino acids 1-241, with some variation between the protomers in the number of resolved amino acids in the termini. The positions for the majority of side chains can be assigned, as well as the presence of two cadmium ions.

As expected, AQP2 shares the common aquaporins fold (Figure 20A-B), but the structure contains some notable differences compared to previous mammalian AQP structures. The initially most prominent feature when solving the AQP2 structure was the binding of the two cadmium ions (referred to as Cd1 and Cd2) and the arrangement of loop D, that were strikingly different from the initial model, based on AQP5. It was also immediately obvious that the C-terminus was not positioned as in other eukaryotic aquaporins.

4.1.3.1 Cd^{2+} binding

Cd^{2+} binding and loop D conformations are tightly connected as described previously (Figure 20C). The Cd1 ion is ligated by protomer A's Glu 155 in loop D, and Gln 57 from TM2 of protomer D (Figure 20D). The octaedric coordination shell is completed by three water molecules. Cd2 is also coordinated by three water molecules, in addition to two residues from protomer C: His 80 in loop B and Glu 232 from the C-terminus (Figure 20E). A very interesting issue here is of course whether the observed cadmium binding is physiologically relevant or just a crystallographic artefact. This is especially intriguing in the light of the experiences from SoPIP2;1, where the situation was very similar: The crystallization was much improved by using cadmium as an additive, and this metal was found occupying a specific binding site at a crucial position within the structure. The idea that this would be replaced by calcium *in vivo* could be put into a convincing experimental context (se section 3.2.3.1). In the case of AQP2, there is to our knowledge no published record of calcium interacting directly with AQP2, even though its role for regulation has been studied [145, 156]. However, attempts to bind radioactively labelled Ca^{2+} to AQP2 expressing oocytes indicate that there actually is a specific interaction (Figure 20F). It is a very interesting perspective that the Cd^{2+}-binding sites in our structure could be Ca^{2+}-binding in the physiological context. As calcium is an important cell signalling molecule with very diverse functions, many roles in relation to function and regulation can be thought. For example, the intracellular levels of Ca^{2+} have been shown to rise at the same time as vasopressin is released [145].

4.1.3.2 C-terminal helix show different conformations

The C-terminal helix of all structurally determined eukaryotic aquaporins overlay well in their structural position. By contrast, the four C-termini of AQP2 all point in different directions (Figure 21A). The ability of the C-terminus to adopt these positions could be linked to two consecutive prolines, Pro 225 and 226, situated in the linker connecting the last TM helix to the C-terminal helix. Proline are common in hinge regions [157] and as none of the other

human aquaporins share this sequence feature, this flexibility seems to be a trait specific for AQP2. This could perhaps be important for AQP2:s possibilities to interact with other proteins, for example the lysosomal protein LIP5, which has been shown to interact directly with this proximal part of the C-terminal region [149]. LIP5 is important for the sorting of endocytosed proteins into multilvesicular bodies (MVB:s) for degradation. Interestingly, yeast two hybrid analysis has shown that the leucines in the C-terminal helix are of importance for the AQP2-LIP5 interaction [Peter Deen, personal communication]. Specifically, Leu 230, 234 and 237 were identified as being involved in LIP5-binding, all which line up on the side of the helix being exposed to the cytoplasm. In the case of the helix of protomer C, which is interacting with the intracellular face of a symmetry-related protomer, these leucines are buried deep within the binding pocket. By contrast, mutating Glu 232, Val 40 or Leu 240, pointing in other directions, had no effect upon LIP5 binding.

One could speculate on whether the interaction seen in the structure, where the C-terminal helix is interacting with AQP2 itself, is relevant for the *in vivo* situation. As it is seen in the crystal, this is obviously not the case, since aquaporins tetramers are not packed against each other in this way when present in the cell membrane. However, it can be noted that the C-terminus of protomer A can be rearranged to fit in the binding pocket of protomer D belonging to the same tetramer in exactly the orientation that is seen in the crystal structure (Figure 21B). Experiments to find evidence for this interaction and its possible functional role are yet to be conducted.

The degree of helical structure and crystallographic order of the C-terminus varies between the AQP2 protomers going from very well resolved in C and then decreasing from A to D to B. The extent of helix formation and quality of electron density seem to depend upon the amount of contact that the helix can form with other parts of the protein. In protomer C, the highly ordered helix is buried in a defined binding pocket as described above. In protomer A, with the second most well defined electron density, one side of the helix lines up against both the N-terminus of protomer D in the same tetramer, and parts from symmetry-related tetramer. The contacts in protomer D and B are less extensive. Thus, it seems as if the formation of the C-terminal helix requires a stabilization in form of an interaction partner.

4.1.3.3 N-termini in two variants

The eukaryotic aquaporins solved previously displays two different conformations in the N-terminus, but the conformation has always been the same between the protomers of the same protein. The N-terminus of AQP2 can be resolved in two protomers, A and D, and these protomers take on one of these conformations each (Figure 21C). Protomer D is reminiscent of AQP1 and several other mammalian AQP structures. In protomer A, the conformation is shared with AQP5 and SoPIP2;1, and is stabilized by interactions with conserved residues in loop B [35]. Interestingly, SoPIP2;1 shows the same type of conformational flexibility in this region as AQP2, as it goes from being AQP5-like in the wild type structure, to being AQP1-like in the phosphomimicking S115E structure (Figure 9A). Thus, it seems as if aquaporins are governed by similar structural principles across the kingdoms of life.

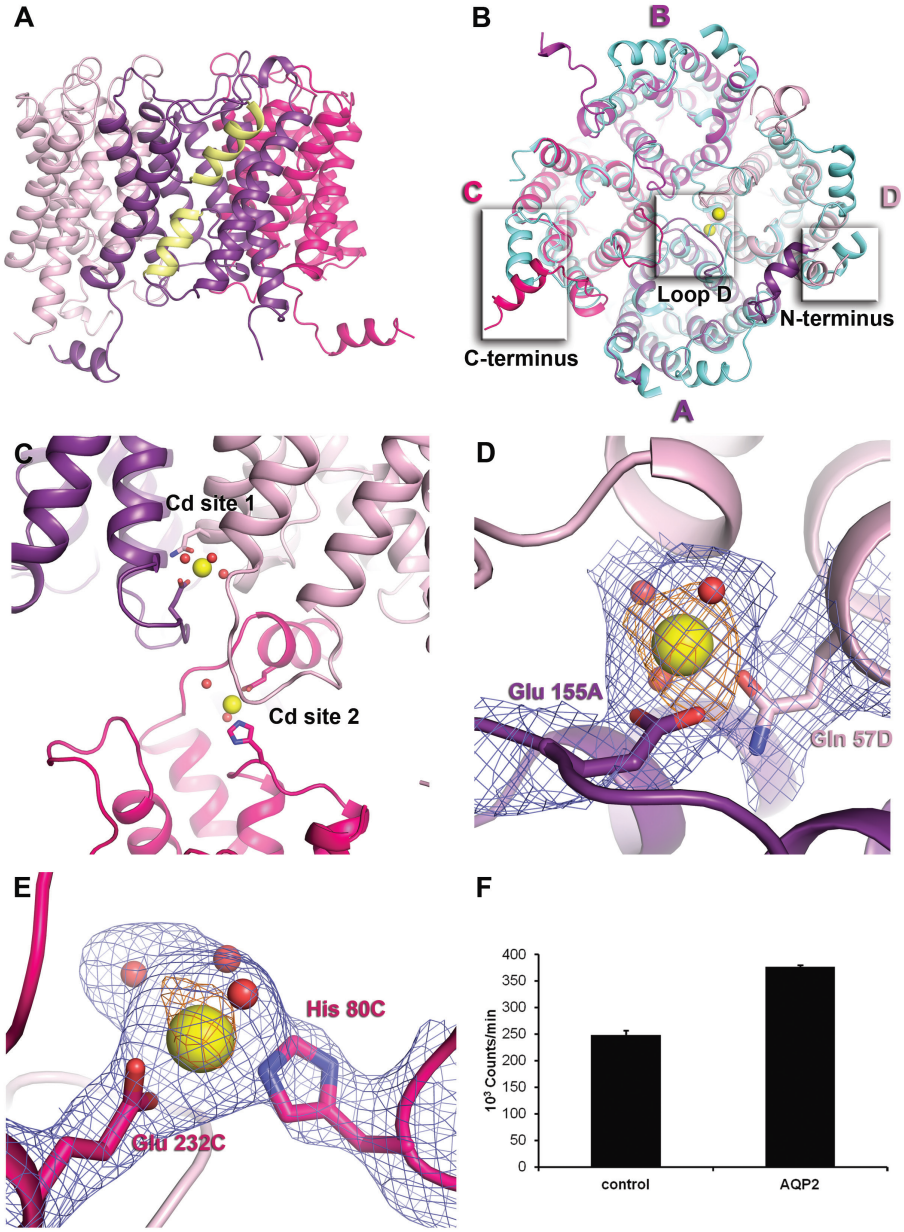

Figure 20. A) The AQP2 tetramer from the side. The half helices of the closest protomer are coloured yellow. B) The AQP2 tetramer from the intracellular side showing protomer A (purple), B (magenta), C (pink) and D (light pink) and Cd^{2+} ions in yellow. Overlay with AQP5 (light blue).The boxes highlight areas with significant structural variations. C) Overview of the Cd-binding sites. The C-terminal helix of protomer C (pink) is interacting with a symmetry related tetramer. Water is shown as red spheres. D) Electron density for the Cd1 site. $2F^{obs}$-F^{calc} map at 1σ (blue) and anomalous map at 3.5σ (orange). E) Electron density for the Cd2 site. F) Binding of radioactive Ca^{2+} is significantly stronger in AQP2-injected oocytes compared to the control.

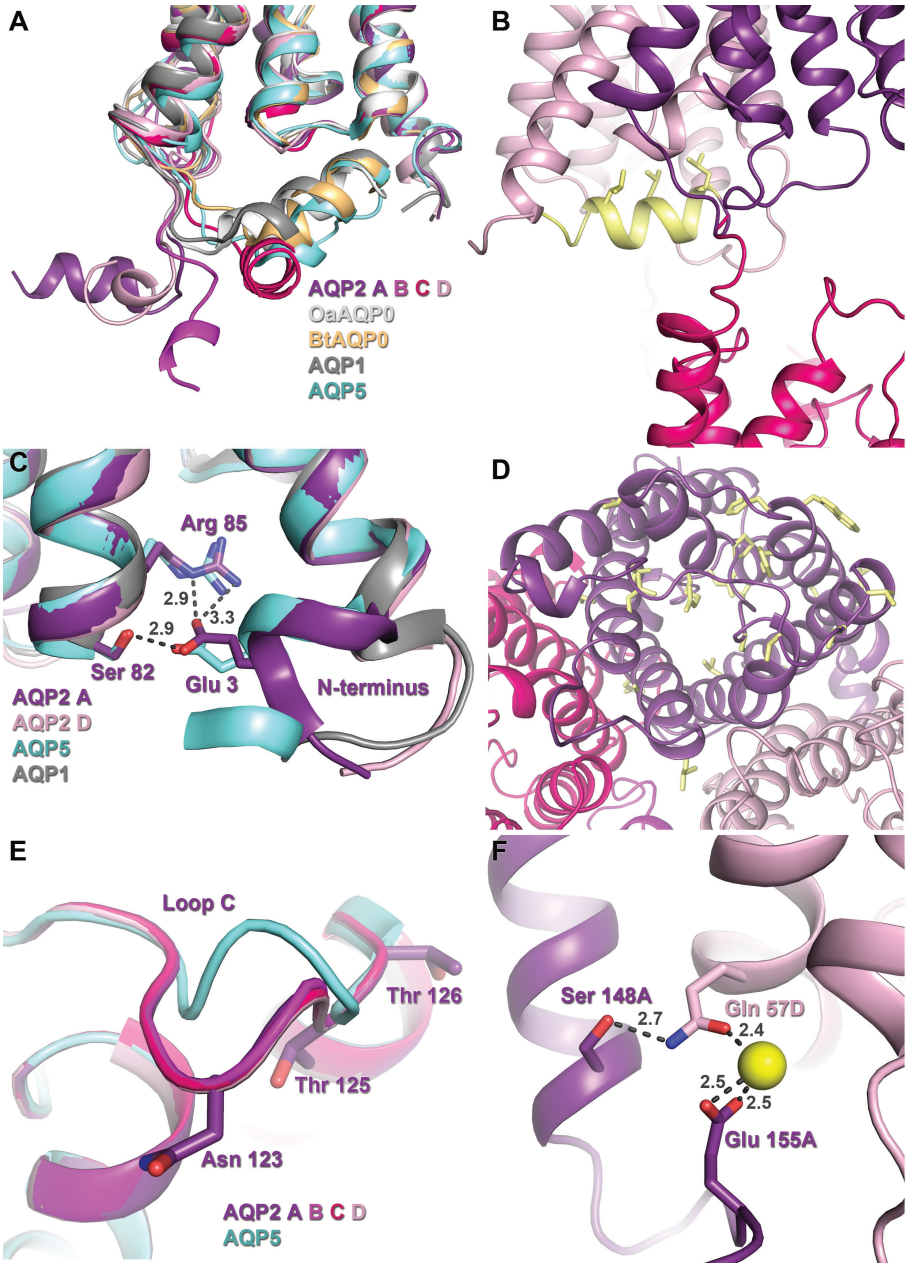

Figure 21. A) C-terminal comparison for AQP2 and other eukaryotic aquaporins. B) The C-terminal helix (yellow) of protomer C (pink) in its interaction pocket in protomer D (light pink) of a neighbouring tetramer. Three leucines line up on one side of the helix. The C-terminal helix is also be modelled to belong to protomer A (purple) of the same tetramer, while remaining in exactly the same position. C) Variable structure of the N-termini. D) Extracellular view of the protomer with NDI-mutations marked in yellow. E) AQP2 differs from other eukaryotic AQP:s in loop C, here represented by AQP5. F) The structure around the Cd1 site is sensitive to mutations. Distances are in Å.

4.1.3.4 NDI mutations in the structural context

As mentioned in section 4.1.1.2, mutations in the AQP2 gene lead to nephrogenic diabetes insipidus. The reason in most cases is that the protein is recognized as defect by the ER quality control system, and is thus retained and degraded by the ER associated degradation pathway (ERAD). The position of these NDI mutations can now be determined. As seen from Figure 21D, the mutations are scattered around the protein, and no unifying theme can be found. Most probably, such a theme can never be identified as there are many reasons as to why proteins are retained in the ER, including exposed hydrophobic patches, immature glycosylation and incomplete oligomerization [158, 159].

In one respect, some conclusions can be drawn concerning why some AQP2 mutants are ER retained. AQP2 harbours an N-glycosylation site towards the end of its extracellular loop C. The recognition sequence for N-linked glycosylation is Asn-X-Ser/Thr with the glycan being attached to the asparagine. In the case of AQP2, this residue corresponds to Asn 123 and is followed by Ser 124 and Thr 125 (Figure 15). No glycosylation is visible in the structure, but exactly in this location, the conformation differs markedly from the other eukaryotic aquaporins (Figure 21E). In oocytes, the glycosylated form of AQP2 is often retained in the ER, but in other cell types, glycosylation is required for proper membrane targeting. Thus, the effect is heavily dependent on the conditions used for study, and the role in the native environment is yet uncertain (Moeller 2011). In the ERAD context, proteins with insufficiently trimmed glycans are retained, and hydrophobic patches in the vicinity are recognized [159]. Mutations of the two consecutive threonines at position 125 and 126 to methionine cause NDI [160, 161]. Thr 125 is part of the glycosylation site itself which is thus disrupted, and at position 126 the mutation confers increased hydrophobicity. Thus, factors related to the improper glycosylation might be the cause of NDI in these cases.

Another cluster of mutations can be noted close to the Cd1 site (Figure 21F). In particular, Q57P and A147T mutants of AQP2 are prevented to leave the ER and cause NDI in patients [161, 162]. Moreover, the mutant S148D that was studied in oocytes is also ER retained [163]. Both Q57 and S148 can be directly linked to the Cd-site and A147 is in its immediate vicinity. Although the physiological relevance of this Cd-site is uninvestigated, it is interesting to note that this specific region seem to be very sensitive for perturbations.

All in all, the new AQP2 structures display features that are distinctively different from other human aquaporins. This gives inspiration to investigate new aspects of AQP2, both as an individual protein and in its relation to other parts of the cell machinery.

5 Future Perspectives

This thesis has focused on the structure and function of two eukaryotic aquaporins and discussed how the events at the molecular level can be coupled to large-scale effects experienced by the individual the human or plant. Our understanding is not yet complete, and there are several lines of research to explore further.

For AQP2, the investigation of structural details has only just started. Since the current structure at 2.95Å was solved from a crystallization condition discovered very recently, there is good potential that the current resolution limit can be further improved by fine-tuning the crystallization parameters. Beyond this, there are several questions that further structural studies of AQP2 could help answering:

The life cycle of AQP2, or any type of membrane protein, contains numerous steps of sorting that decides the future fate of the molecule. Beginning at the birth in the ER (Is this molecule of high enough quality?), AQP2 sorting continues through its active life while trafficked in the cell (Is water transport needed right now?) until its degradation (Is this molecule useful anymore?). There is quite some knowledge about which accessory proteins that participate in this process, but what structural features they actually recognize and act upon is very unclear. For AQP2, there is an overwhelming amount of mutational data, both from patients suffering from nephrogenic diabetes insipidus, and from different functional investigations carried out in the lab. The effects of many of these mutations are related to sorting problems. It would be very interesting if this knowledge, together with future AQP2 structures, could improve our understanding of these types of processes at the structural level.

The recessive NDI mutations in the core protein causes functional failure as these protein molecules are recognized as faulty by the ER protein quality control machinery. Single mutations at these sites could be enlightening, as well as complexes with crucial interaction partners.

The final part of the C-terminus is crucial for many aspects of AQP2 regulation, but is lacking from the current structure. It would of course be extremely interesting to have structural information about it. How are for example contacts mediated to the trafficking and degradation machinery? However, this would likely require a completely different strategy where high levels of homogenous full length protein could be achieved. This material could be then co-crystallised with an interacting protein that could lock up the flexible C-terminus in a defined conformation.

Compared to AQP2, the molecular conformation of SoPIP2; is well-known, but it remains to discern the structural details of channel opening to a better resolution. Hopefully, data on the S188E mutant can provide this. Also, our speculation on mechanosensitive gating need to be further characterised.

To date, SoPIP2;1 is the only structurally determined plant aquaporin. Given the large number of isoforms in plants, small differences is obviously of great value for the organism. Structures of plant aquaporins with different substrate specificities would be interesting and large questions remain e.g. in relation to the gas transporting ability of some isoforms.

In most aspects, the aquaporins are alike, but evolution has still kept them somewhat different. Understanding these subtle dissimilarities helps us understand the fundamentals of our biology and is also important if the aquaporins are to be used as drug targets. Therefore, structural research on aquaporins still has many questions to answer.

6 References

1. Fagerberg, L., et al., *Prediction of the human membrane proteome.* Proteomics, 2010. **10**(6): p. 1141-9.
2. von Heijne, G., *The membrane protein universe: what's out there and why bother?* Journal of internal medicine, 2007. **261**(6): p. 543-57.
3. Kendrew, J.C., et al., *Structure of myoglobin: A three-dimensional Fourier synthesis at 2 A. resolution.* Nature, 1960. **185**(4711): p. 422-7.
4. Deisenhofer, J., et al., *Structure of the protein subunits in the photosynthetic reaction centre of Rhodopseudomonas viridis at 3A resolution.* Nature, 1985. **318**(6047): p. 618-24.
5. *Protein Data Bank.* 2013-03-07]; Available from: http://www.pdb.org/pdb/statistics/holdings.do.
6. *Membrane Proteins of known 3D Structure.* 2013-03-07]; Available from: http://blanco.biomol.uci.edu/mpstruc/listAll/list.
7. Macey, R.I., *Transport of water and urea in red blood cells.* The American journal of physiology, 1984. **246**(3 Pt 1): p. C195-203.
8. Kachadorian, W.A., J.B. Wade, and V.A. DiScala, *Vasopressin: induced structural change in toad bladder luminal membrane.* Science, 1975. **190**(4209): p. 67-9.
9. Denker, B.M., et al., *Identification, purification, and partial characterization of a novel Mr 28,000 integral membrane protein from erythrocytes and renal tubules.* J Biol Chem, 1988. **263**(30): p. 15634-42.
10. Preston, G.M., et al., *Appearance of water channels in Xenopus oocytes expressing red cell CHIP28 protein.* Science, 1992. **256**(5055): p. 385-7.
11. Smith, B.L. and P. Agre, *Erythrocyte Mr 28,000 transmembrane protein exists as a multisubunit oligomer similar to channel proteins.* The Journal of biological chemistry, 1991. **266**(10): p. 6407-15.
12. Agre, P., S. Sasaki, and M.J. Chrispeels, *Aquaporins: a family of water channel proteins.* Am J Physiol, 1993. **265**(3 Pt 2): p. F461.
13. Murata, K., et al., *Structural determinants of water permeation through aquaporin-1.* Nature, 2000. **407**(6804): p. 599-605.
14. Fu, D., et al., *Structure of a glycerol-conducting channel and the basis for its selectivity.* Science, 2000. **290**(5491): p. 481-6.
15. Gorin, M.B., et al., *The major intrinsic protein (MIP) of the bovine lens fiber membrane: characterization and structure based on cDNA cloning.* Cell, 1984. **39**(1): p. 49-59.
16. Preston, G.M. and P. Agre, *Isolation of the cDNA for erythrocyte integral membrane protein of 28 kilodaltons: member of an ancient channel family.* Proceedings of the National Academy of Sciences of the United States of America, 1991. **88**(24): p. 11110-4.
17. Jung, J.S., et al., *Molecular characterization of an aquaporin cDNA from brain - candidate osmoreceptor and regulator of water-balance.* Proceedings of the National Academy of Sciences of the United States of America, 1994. **91**(26): p. 13052-13056.
18. Cheng, A., et al., *Three-dimensional organization of a human water channel.* Nature, 1997. **387**(6633): p. 627-30.
19. Sui, H., et al., *Structural basis of water-specific transport through the AQP1 water channel.* Nature, 2001. **414**(6866): p. 872-8.
20. Lee, J.K., et al., *Structural basis for conductance by the archaeal aquaporin AqpM at 1.68 A.* Proceedings of the National Academy of Sciences of the United States of America, 2005. **102**(52): p. 18932-7.
21. Newby, Z.E., et al., *Crystal structure of the aquaglyceroporin PfAQP from the malarial parasite Plasmodium falciparum.* Nature structural & molecular biology, 2008. **15**(6): p. 619-25.
22. Savage, D.F., et al., *Structural context shapes the aquaporin selectivity filter.* Proceedings of the National Academy of Sciences of the United States of America, 2010. **107**(40): p. 17164-9.
23. de Groot, B.L. and H. Grubmuller, *The dynamics and energetics of water permeation and proton exclusion in aquaporins.* Curr Opin Struct Biol, 2005. **15**(2): p. 176-83.
24. Burykin, A. and A. Warshel, *On the origin of the electrostatic barrier for proton transport in aquaporin.* FEBS Lett, 2004. **570**(1-3): p. 41-6.
25. Li, H., et al., *Enhancement of proton conductance by mutations of the selectivity filter of aquaporin-1.* Journal of Molecular Biology, 2011. **407**(4): p. 607-20.

26. Harries, W.E., et al., *The channel architecture of aquaporin 0 at a 2.2-A resolution.* Proceedings of the National Academy of Sciences of the United States of America, 2004. **101**(39): p. 14045-50.
27. Gonen, T., et al., *Aquaporin-0 membrane junctions reveal the structure of a closed water pore.* Nature, 2004. **429**(6988): p. 193-7.
28. Gonen, T., et al., *Lipid-protein interactions in double-layered two-dimensional AQP0 crystals.* Nature, 2005. **438**(7068): p. 633-8.
29. Hite, R.K., Z. Li, and T. Walz, *Principles of membrane protein interactions with annular lipids deduced from aquaporin-0 2D crystals.* The EMBO journal, 2010. **29**(10): p. 1652-8.
30. Ren, G., et al., *Visualization of a water-selective pore by electron crystallography in vitreous ice.* Proceedings of the National Academy of Sciences of the United States of America, 2001. **98**(4): p. 1398-403.
31. de Groot, B.L., A. Engel, and H. Grubmuller, *A refined structure of human aquaporin-1.* Febs Letters, 2001. **504**(3): p. 206-11.
32. Ho, J.D., et al., *Crystal structure of human aquaporin 4 at 1.8 A and its mechanism of conductance.* Proceedings of the National Academy of Sciences of the United States of America, 2009. **106**(18): p. 7437-42.
33. Hiroaki, Y., et al., *Implications of the aquaporin-4 structure on array formation and cell adhesion.* Journal of Molecular Biology, 2006. **355**(4): p. 628-39.
34. Tani, T., et al., *Immunolocalization of aquaporin-8 in rat digestive organs and testis.* Archives of histology and cytology, 2001. **64**(2): p. 159-68.
35. Horsefield, R., et al., *High-resolution x-ray structure of human aquaporin 5.* Proceedings of the National Academy of Sciences of the United States of America, 2008. **105**(36): p. 13327-32.
36. Tornroth-Horsefield, S., et al., *Structural mechanism of plant aquaporin gating.* Nature, 2006. **439**(7077): p. 688-94.
37. Nyblom, M., et al., *Structural and functional analysis of SoPIP2;1 mutants adds insight into plant aquaporin gating.* J Mol Biol, 2009. **387**(3): p. 653-68.
38. Fischer, G., et al., *Crystal structure of a yeast aquaporin at 1.15 angstrom reveals a novel gating mechanism.* PLoS Biol, 2009. **7**(6): p. e1000130.
39. Savage, D.F., et al., *Architecture and selectivity in aquaporins: 2.5 a X-ray structure of aquaporin Z.* PLoS biology, 2003. **1**(3): p. E72.
40. Jiang, J., B.V. Daniels, and D. Fu, *Crystal structure of AqpZ tetramer reveals two distinct Arg-189 conformations associated with water permeation through the narrowest constriction of the water-conducting channel.* The Journal of biological chemistry, 2006. **281**(1): p. 454-60.
41. Savage, D.F. and R.M. Stroud, *Structural basis of aquaporin inhibition by mercury.* Journal of molecular biology, 2007. **368**(3): p. 607-17.
42. Tajkhorshid, E., et al., *Control of the selectivity of the aquaporin water channel family by global orientational tuning.* Science, 2002. **296**(5567): p. 525-30.
43. Grisshammer, R., *Understanding recombinant expression of membrane proteins.* Current opinion in biotechnology, 2006. **17**(4): p. 337-40.
44. Grisshammer, R. and C.G. Tate, *Overexpression of integral membrane proteins for structural studies.* Quarterly reviews of biophysics, 1995. **28**(3): p. 315-422.
45. Bill, R.M., et al., *Overcoming barriers to membrane protein structure determination.* Nature biotechnology, 2011. **29**(4): p. 335-40.
46. Cregg, J.M., *Introduction: distinctions between Pichia pastoris and other expression systems.* Methods in molecular biology, 2007. **389**: p. 1-10.
47. Cereghino, G.P., et al., *Production of recombinant proteins in fermenter cultures of the yeast Pichia pastoris.* Current opinion in biotechnology, 2002. **13**(4): p. 329-32.
48. Ramon, A. and M. Marin, *Advances in the production of membrane proteins in Pichia pastoris.* Biotechnology journal, 2011. **6**(6): p. 700-6.
49. le Maire, M., P. Champeil, and J.V. Moller, *Interaction of membrane proteins and lipids with solubilizing detergents.* Biochimica et biophysica acta, 2000. **1508**(1-2): p. 86-111.
50. Prive, G.G., *Detergents for the stabilization and crystallization of membrane proteins.* Methods, 2007. **41**(4): p. 388-97.
51. Newstead, S., S. Ferrandon, and S. Iwata, *Rationalizing alpha-helical membrane protein crystallization.* Protein science : a publication of the Protein Society, 2008. **17**(3): p. 466-72.
52. Kunji, E.R., et al., *Determination of the molecular mass and dimensions of membrane proteins by size exclusion chromatography.* Methods, 2008. **46**(2): p. 62-72.
53. Zhang, H. and W.A. Cramer, *Problems in obtaining diffraction-quality crystals of hetero-oligomeric integral membrane proteins.* Journal of structural and functional genomics, 2005. **6**(2-3): p. 219-23.

54. Chae, P.S., et al., *Glucose-Neopentyl Glycol (GNG) amphiphiles for membrane protein study.* Chemical communications, 2012.
55. Chae, P.S., et al., *Maltose-neopentyl glycol (MNG) amphiphiles for solubilization, stabilization and crystallization of membrane proteins.* Nature methods, 2010. **7**(12): p. 1003-8.
56. *Affymetrix.* 2013-03-07]; Available from: http://www.affymetrix.com/estore/browse/brand/anatrace/product.jsp?productId=prod430001&categoryId=35873&productName=Octyl-Glucose-Neopentyl-Glycol#1_3.
57. Asherie, N., *Protein crystallization and phase diagrams.* Methods, 2004. **34**(3): p. 266-72.
58. Landau, E.M. and J.P. Rosenbusch, *Lipidic cubic phases: a novel concept for the crystallization of membrane proteins.* Proc Natl Acad Sci U S A, 1996. **93**(25): p. 14532-5.
59. Wohri, A.B., et al., *A lipidic-sponge phase screen for membrane protein crystallization.* Structure, 2008. **16**(7): p. 1003-9.
60. Faham, S. and J.U. Bowie, *Bicelle crystallization: a new method for crystallizing membrane proteins yields a monomeric bacteriorhodopsin structure.* Journal of Molecular Biology, 2002. **316**(1): p. 1-6.
61. Steyaert, J. and B.K. Kobilka, *Nanobody stabilization of G protein-coupled receptor conformational states.* Current opinion in structural biology, 2011.
62. Hunte, C. and H. Michel, *Crystallisation of membrane proteins mediated by antibody fragments.* Current opinion in structural biology, 2002. **12**(4): p. 503-8.
63. Chun, E., et al., *Fusion partner toolchest for the stabilization and crystallization of G protein-coupled receptors.* Structure, 2012. **20**(6): p. 967-76.
64. Garman, E.F. and R.L. Owen, *Cryocooling and radiation damage in macromolecular crystallography.* Acta Crystallogr D Biol Crystallogr, 2006. **62**(Pt 1): p. 32-47.
65. Brunger, A.T., *Free R value: a novel statistical quantity for assessing the accuracy of crystal structures.* Nature, 1992. **355**(6359): p. 472-5.
66. Rigaud, J.L., *Membrane proteins: functional and structural studies using reconstituted proteoliposomes and 2-D crystals.* Brazilian journal of medical and biological research = Revista brasileira de pesquisas medicas e biologicas / Sociedade Brasileira de Biofisica ... [et al.], 2002. **35**(7): p. 753-66.
67. Geertsma, E.R., et al., *Membrane reconstitution of ABC transporters and assays of translocator function.* Nature protocols, 2008. **3**(2): p. 256-66.
68. van Heeswijk, M.P. and C.H. van Os, *Osmotic water permeabilities of brush border and basolateral membrane vesicles from rat renal cortex and small intestine.* J Membr Biol, 1986. **92**(2): p. 183-93.
69. Maurel, C., et al., *Plant aquaporins: membrane channels with multiple integrated functions.* Annual review of plant biology, 2008. **59**: p. 595-624.
70. Kaldenhoff, R., et al., *Aquaporins and plant water balance.* Plant, cell & environment, 2008. **31**(5): p. 658-66.
71. Johanson, U., et al., *The complete set of genes encoding major intrinsic proteins in Arabidopsis provides a framework for a new nomenclature for major intrinsic proteins in plants.* Plant physiology, 2001. **126**(4): p. 1358-69.
72. Sakurai, J., et al., *Identification of 33 rice aquaporin genes and analysis of their expression and function.* Plant & cell physiology, 2005. **46**(9): p. 1568-77.
73. Danielson, J.A. and U. Johanson, *Unexpected complexity of the aquaporin gene family in the moss Physcomitrella patens.* BMC Plant Biol, 2008. **8**: p. 45.
74. Wudick, M.M., D.T. Luu, and C. Maurel, *A look inside: localization patterns and functions of intracellular plant aquaporins.* The New phytologist, 2009. **184**(2): p. 289-302.
75. Maurel, C., et al., *The cellular dynamics of plant aquaporin expression and functions.* Current opinion in plant biology, 2009. **12**(6): p. 690-8.
76. Johansson, I., et al., *The major integral proteins of spinach leaf plasma membranes are putative aquaporins and are phosphorylated in response to Ca2+ and apoplastic water potential.* The Plant cell, 1996. **8**(7): p. 1181-91.
77. Chaumont, F., et al., *Plasma membrane intrinsic proteins from maize cluster in two sequence subgroups with differential aquaporin activity.* Plant Physiol, 2000. **122**(4): p. 1025-34.
78. Otto, B., et al., *Aquaporin tetramer composition modifies the function of tobacco aquaporins.* The Journal of biological chemistry, 2010. **285**(41): p. 31253-60.
79. Zelazny, E., et al., *FRET imaging in living maize cells reveals that plasma membrane aquaporins interact to regulate their subcellular localization.* Proceedings of the National Academy of Sciences of the United States of America, 2007. **104**(30): p. 12359-64.
80. Alleva, K., et al., *Plasma membrane of Beta vulgaris storage root shows high water channel activity regulated by cytoplasmic pH and a dual range of calcium concentrations.* Journal of Experimental Botany, 2006. **57**(3): p. 609-621.

81. Gerbeau, P., et al., *The water permeability of Arabidopsis plasma membrane is regulated by divalent cations and pH.* The Plant journal : for cell and molecular biology, 2002. **30**(1): p. 71-81.
82. Verdoucq, L., A. Grondin, and C. Maurel, *Structure-function analysis of plant aquaporin AtPIP2;1 gating by divalent cations and protons.* The Biochemical journal, 2008. **415**(3): p. 409-16.
83. Johansson, I., et al., *Water transport activity of the plasma membrane aquaporin PM28A is regulated by phosphorylation.* The Plant cell, 1998. **10**(3): p. 451-9.
84. Van Wilder, V., et al., *Maize plasma membrane aquaporins belonging to the PIP1 and PIP2 subgroups are in vivo phosphorylated.* Plant & cell physiology, 2008. **49**(9): p. 1364-77.
85. Maurel, C., et al., *Phosphorylation regulates the water channel activity of the seed-specific aquaporin alpha-TIP.* The EMBO journal, 1995. **14**(13): p. 3028-35.
86. Aroca, R., et al., *The role of aquaporins and membrane damage in chilling and hydrogen peroxide induced changes in the hydraulic conductance of maize roots.* Plant Physiol, 2005. **137**(1): p. 341-53.
87. Sjovall-Larsen, S., et al., *Purification and characterization of two protein kinases acting on the aquaporin SoPIP2;1.* Biochimica et biophysica acta, 2006. **1758**(8): p. 1157-64.
88. Prak, S., et al., *Multiple phosphorylations in the C-terminal tail of plant plasma membrane aquaporins: role in subcellular trafficking of AtPIP2;1 in response to salt stress.* Molecular & cellular proteomics : MCP, 2008. **7**(6): p. 1019-30.
89. Nuhse, T.S., et al., *Phosphoproteomics of the Arabidopsis plasma membrane and a new phosphorylation site database.* The Plant cell, 2004. **16**(9): p. 2394-405.
90. Casado-Vela, J., et al., *Analysis of root plasma membrane aquaporins from Brassica oleracea: post-translational modifications, de novo sequencing and detection of isoforms by high resolution mass spectrometry.* Journal of proteome research, 2010. **9**(7): p. 3479-94.
91. Guenther, J.F., et al., *Phosphorylation of soybean nodulin 26 on serine 262 enhances water permeability and is regulated developmentally and by osmotic signals.* The Plant cell, 2003. **15**(4): p. 981-91.
92. Amezcua-Romero, J.C., O. Pantoja, and R. Vera-Estrella, *Ser123 is essential for the water channel activity of McPIP2;1 from Mesembryanthemum crystallinum.* The Journal of biological chemistry, 2010. **285**(22): p. 16739-47.
93. Groban, E.S., A. Narayanan, and M.P. Jacobson, *Conformational changes in protein loops and helices induced by post-translational phosphorylation.* PLoS computational biology, 2006. **2**(4): p. e32.
94. Santoni, V., et al., *Methylation of aquaporins in plant plasma membrane.* Biochem J, 2006. **400**(1): p. 189-97.
95. Hachez, C., et al., *Insights into plant plasma membrane aquaporin trafficking.* Trends in plant science, 2013.
96. Felle, H.H., *pH: Signal and messenger in plant cells.* Plant Biology, 2001. **3**(6): p. 577-591.
97. Fischer, M. and R. Kaldenhoff, *On the pH regulation of plant aquaporins.* The Journal of biological chemistry, 2008. **283**(49): p. 33889-92.
98. Sutka, M., et al., *Natural variation of root hydraulics in Arabidopsis grown in normal and salt-stressed conditions.* Plant physiology, 2011. **155**(3): p. 1264-76.
99. Tournaire-Roux, C., et al., *Cytosolic pH regulates root water transport during anoxic stress through gating of aquaporins.* Nature, 2003. **425**(6956): p. 393-7.
100. Yasui, M., et al., *Rapid gating and anion permeability of an intracellular aquaporin.* Nature, 1999. **402**(6758): p. 184-7.
101. Hirano, Y., et al., *Molecular Mechanisms of How Mercury Inhibits Water Permeation through Aquaporin-1: Understanding by Molecular Dynamics Simulation.* Biophysical Journal, 2010. **98**(8): p. 1512-1519.
102. Zhao, H.B., Z.B. Zhang, and P. Xu, *Enhanced aquaporin activity of two different genotypes of drought-resistant wheat (Triticum aestivum L.) cultivars facilitate their adaptation to drought stress.* Journal of Food Agriculture & Environment, 2010. **8**(2): p. 1158-1161.
103. Ionenko, I.F. and A.V. Anisimov, *Radial diffusion transport of water in various zones of maize root and its sensitivity to mercury chloride.* Russian Journal of Plant Physiology, 2007. **54**(2): p. 224-229.
104. Daniels, M.J., et al., *Characterization of a new vacuolar membrane aquaporin sensitive to mercury at a unique site.* The Plant cell, 1996. **8**(4): p. 587-99.
105. Secchi, F., et al., *Functional analysis of putative genes encoding the PIP2 water channel subfamily in Populus trichocarpa.* Tree Physiology, 2009. **29**(11): p. 1467-1477.
106. Suga, S. and M. Maeshima, *Water channel activity of radish plasma membrane aquaporins heterologously expressed in yeast and their modification by site-directed mutagenesis.* Plant and Cell Physiology, 2004. **45**(7): p. 823-830.
107. Kammerloher, W., et al., *Water channels in the plant plasma membrane cloned by immunoselection from a mammalian expression system.* The Plant journal : for cell and molecular biology, 1994. **6**(2): p. 187-99.

108. Daniels, M.J., T.E. Mirkov, and M.J. Chrispeels, *The plasma-membrane of Arabidopsis thaliana contains a mercury-insensitive aquaporin that is a homolog of the tonoplast water channel protein TIP.* Plant physiology, 1994. **106**(4): p. 1325-1333.
109. Biela, A., et al., *The Nicotiana tabacum plasma membrane aquaporin NtAQP1 is mercury-insensitive and permeable for glycerol.* Plant Journal, 1999. **18**(5): p. 565-570.
110. Bienert, G.P., et al., *A conserved cysteine residue is involved in disulphide bond formation between plant plasma membrane aquaporin monomers.* The Biochemical journal, 2012.
111. Krajinski, F., et al., *Arbuscular mycorrhiza development regulates the mRNA abundance of Mtaqp1 encoding a mercury-insensitive aquaporin of Medicago truncatula.* Planta, 2000. **211**(1): p. 85-90.
112. Delnomdedieu, M., et al., *Specific interactions of mercury chloride with membranes and other ligands as revealed by mercury-NMR.* Chemico-biological interactions, 1992. **81**(3): p. 243-69.
113. Lande, M.B., J.M. Donovan, and M.L. Zeidel, *The relationship between membrane fluidity and permeabilities to water, solutes, ammonia, and protons.* The Journal of general physiology, 1995. **106**(1): p. 67-84.
114. Tong, J., M.M. Briggs, and T.J. McIntosh, *Water permeability of aquaporin-4 channel depends on bilayer composition, thickness, and elasticity.* Biophysical Journal, 2012. **103**(9): p. 1899-908.
115. Levitan, I., et al., *Membrane cholesterol content modulates activation of volume-regulated anion current in bovine endothelial cells.* The Journal of general physiology, 2000. **115**(4): p. 405-16.
116. Subbaiah, C.C., D.S. Bush, and M.M. Sachs, *Elevation of cytosolic calcium precedes anoxic gene expression in maize suspension-cultured cells.* The Plant cell, 1994. **6**(12): p. 1747-62.
117. Chen, J. and Z.M. Yang, *Mercury toxicity, molecular response and tolerance in higher plants.* Biometals, 2012. **25**(5): p. 847-57.
118. Lin, Y.F. and M.G. Aarts, *The molecular mechanism of zinc and cadmium stress response in plants.* Cellular and molecular life sciences : CMLS, 2012. **69**(19): p. 3187-206.
119. Poschenrieder CH, B.J., *Water relations in heavy metal stress*, in *Heavy metal stress in plants. From biomolecules to ecosystems*, P. MNV, Editor 2004, Springer: Berlin. p. 249-270.
120. Przedpelska-Wasowicz, E.M. and M. Wierzbicka, *Gating of aquaporins by heavy metals in Allium cepa L. epidermal cells.* Protoplasma, 2011. **248**(4): p. 663-71.
121. Herrera, M. and J.L. Garvin, *Aquaporins as gas channels.* Pflugers Archiv : European journal of physiology, 2011. **462**(4): p. 623-30.
122. Boron, W.F., *Sharpey-Schafer lecture: gas channels.* Exp Physiol, 2010. **95**(12): p. 1107-30.
123. Uehlein, N., et al., *The Arabidopsis aquaporin PIP1;2 rules cellular CO(2) uptake.* Plant, cell & environment, 2011.
124. de Groot, B.L. and J.S. Hub, *A decade of debate: significance of CO2 permeation through membrane channels still controversial.* Chemphyschem : a European journal of chemical physics and physical chemistry, 2011. **12**(5): p. 1021-2.
125. Kaldenhoff, R., *Mechanisms underlying CO2 diffusion in leaves.* Current opinion in plant biology, 2012. **15**(3): p. 276-81.
126. Uehlein, N., et al., *Function of Nicotiana tabacum aquaporins as chloroplast gas pores challenges the concept of membrane CO2 permeability.* The Plant cell, 2008. **20**(3): p. 648-57.
127. Helland, R., et al., *An oxidized tryptophan facilitates copper binding in Methylococcus capsulatus-secreted protein MopE.* The Journal of biological chemistry, 2008. **283**(20): p. 13897-904.
128. Samanta, U., D. Pal, and P. Chakrabarti, *Environment of tryptophan side chains in proteins.* Proteins, 2000. **38**(3): p. 288-300.
129. Yool, A.J. and E.M. Campbell, *Structure, function and translational relevance of aquaporin dual water and ion channels.* Molecular aspects of medicine, 2012. **33**(5-6): p. 553-61.
130. Lee, J.W., et al., *Phosphorylation of nodulin 26 on serine 262 affects its voltage-sensitive channel activity in planar lipid bilayers.* J Biol Chem, 1995. **270**(45): p. 27051-7.
131. Weaver, C.D., et al., *Nodulin 26, a nodule-specific symbiosome membrane protein from soybean, is an ion channel.* The Journal of biological chemistry, 1994. **269**(27): p. 17858-62.
132. Carbrey, J.M. and P. Agre, *Discovery of the aquaporins and development of the field.* Handbook of experimental pharmacology, 2009(190): p. 3-28.
133. Huber, V.J., M. Tsujita, and T. Nakada, *Aquaporins in drug discovery and pharmacotherapy.* Molecular aspects of medicine, 2012. **33**(5-6): p. 691-703.
134. Sasaki, S., *Aquaporin 2: from its discovery to molecular structure and medical implications.* Molecular aspects of medicine, 2012. **33**(5-6): p. 535-46.
135. Hatakeyama, S., et al., *Cloning of a new aquaporin (AQP10) abundantly expressed in duodenum and jejunum.* Biochemical and Biophysical Research Communications, 2001. **287**(4): p. 814-9.

136. Itoh, T., et al., *Identification of a novel aquaporin, AQP12, expressed in pancreatic acinar cells.* Biochemical and Biophysical Research Communications, 2005. **330**(3): p. 832-8.
137. Fushimi, K., et al., *Cloning and expression of apical membrane water channel of rat kidney collecting tubule.* Nature, 1993. **361**(6412): p. 549-52.
138. Kwon, T.H., et al., *Aquaporins in the kidney.* Handbook of experimental pharmacology, 2009(190): p. 95-132.
139. Nielsen, S., et al., *Vasopressin increases water permeability of kidney collecting duct by inducing translocation of aquaporin-CD water channels to plasma membrane.* Proceedings of the National Academy of Sciences of the United States of America, 1995. **92**(4): p. 1013-7.
140. Deen, P.M., et al., *Requirement of human renal water channel aquaporin-2 for vasopressin-dependent concentration of urine.* Science, 1994. **264**(5155): p. 92-5.
141. Moeller, H.B., E.T. Olesen, and R.A. Fenton, *Regulation of the water channel aquaporin-2 by posttranslational modification.* American journal of physiology. Renal physiology, 2011. **300**(5): p. F1062-73.
142. Moeller, H.B., et al., *Phosphorylation of aquaporin-2 regulates its endocytosis and protein-protein interactions.* Proceedings of the National Academy of Sciences of the United States of America, 2010. **107**(1): p. 424-9.
143. Kamsteeg, E.J., et al., *Short-chain ubiquitination mediates the regulated endocytosis of the aquaporin-2 water channel.* Proceedings of the National Academy of Sciences of the United States of America, 2006. **103**(48): p. 18344-9.
144. Loonen, A.J., et al., *Aquaporin 2 mutations in nephrogenic diabetes insipidus.* Seminars in nephrology, 2008. **28**(3): p. 252-65.
145. Nedvetsky, P.I., et al., *Regulation of aquaporin-2 trafficking.* Handbook of experimental pharmacology, 2009(190): p. 133-57.
146. Hoffert, J.D., C.L. Chou, and M.A. Knepper, *Aquaporin-2 in the "-omics" era.* The Journal of biological chemistry, 2009. **284**(22): p. 14683-7.
147. Noda, Y., et al., *Reciprocal interaction with G-actin and tropomyosin is essential for aquaporin-2 trafficking.* The Journal of cell biology, 2008. **182**(3): p. 587-601.
148. Lu, H.A., et al., *Heat shock protein 70 interacts with aquaporin-2 and regulates its trafficking.* The Journal of biological chemistry, 2007. **282**(39): p. 28721-32.
149. van Balkom, B.W., et al., *LIP5 interacts with aquaporin 2 and facilitates its lysosomal degradation.* Journal of the American Society of Nephrology : JASN, 2009. **20**(5): p. 990-1001.
150. Moeller, H.B., S. Rittig, and R.A. Fenton, *Nephrogenic Diabetes Insipidus: Essential Insights into the Molecular Background and Potential Therapies for Treatment.* Endocrine reviews, 2013.
151. Guyon, C., et al., *Characterization of D150E and G196D aquaporin-2 mutations responsible for nephrogenic diabetes insipidus: importance of a mild phenotype.* American journal of physiology. Renal physiology, 2009. **297**(2): p. F489-98.
152. Leduc-Nadeau, A., et al., *New autosomal recessive mutations in aquaporin-2 causing nephrogenic diabetes insipidus through deficient targeting display normal expression in Xenopus oocytes.* The Journal of physiology, 2010. **588**(Pt 12): p. 2205-18.
153. Schenk, A.D., et al., *The 4.5 A structure of human AQP2.* Journal of Molecular Biology, 2005. **350**(2): p. 278-89.
154. Oberg, F., et al., *Insight into factors directing high production of eukaryotic membrane proteins; production of 13 human AQPs in Pichia pastoris.* Mol Membr Biol, 2009. **26**(4): p. 215-27.
155. Kellosalo, J., et al., *The structure and catalytic cycle of a sodium-pumping pyrophosphatase.* Science, 2012. **337**(6093): p. 473-6.
156. Procino, G., et al., *Aquaporin 2 and apical calcium-sensing receptor: new players in polyuric disorders associated with hypercalciuria.* Seminars in nephrology, 2008. **28**(3): p. 297-305.
157. Sansom, M.S.P. and H. Weinstein, *Hinges, swivels and switches: the role of prolines in signalling via transmembrane α-helices.* Trends in Pharmacological Science, 2000. **21**(11): p. 445-451.
158. Vembar, S.S. and J.L. Brodsky, *One step at a time: endoplasmic reticulum-associated degradation.* Nature reviews. Molecular cell biology, 2008. **9**(12): p. 944-57.
159. Brodsky, J.L. and W.R. Skach, *Protein folding and quality control in the endoplasmic reticulum: Recent lessons from yeast and mammalian cell systems.* Current opinion in cell biology, 2011. **23**(4): p. 464-75.
160. Marr, N., et al., *Cell-biologic and functional analyses of five new Aquaporin-2 missense mutations that cause recessive nephrogenic diabetes insipidus.* Journal of the American Society of Nephrology : JASN, 2002. **13**(9): p. 2267-77.

161. Marr, N., et al., *Functionality of aquaporin-2 missense mutants in recessive nephrogenic diabetes insipidus.* Pflugers Archiv : European journal of physiology, 2001. **442**(1): p. 73-7.
162. Lin, S.H., et al., *Two novel aquaporin-2 mutations responsible for congenital nephrogenic diabetes insipidus in Chinese families.* The Journal of clinical endocrinology and metabolism, 2002. **87**(6): p. 2694-700.
163. van Balkom, B.W., et al., *The role of putative phosphorylation sites in the targeting and shuttling of the aquaporin-2 water channel.* The Journal of biological chemistry, 2002. **277**(44): p. 41473-9.

7 Acknowledgements

The time since I first entered the Lundberg Laboratory has passed both enormously fast and enormously slow. Although it feels as if it was yesterday I started my studies, it has been a few years and life is now radically different, both for me and for many others that have shared my time here. I want to thank all the people who helped me at some stage, and in particular I want to mention:

Susanna – jag har haft ofattbar tur som fick dig som handledare. Tack för att ha gett mig allt från vetenskapliga vägledning och support i labbet till oändliga mängder barnkläder och god vänskap. Det behövs fler forskare som du!

Richard – you are both a visionary scientist and a truly warm and generous person. Thank you for giving me the opportunity to work in such an environment.

Gerhard – tack för det goda sällskapet både när vi delade våra fyra m² och besökte andra kontinenter. Och inte minst tack för att du samlade data så att jag fick med AQP2 i avhandlingen – A friend in need is a friend indeed!

Mike – att tvinga dig att bli min exjobbare var kanske ett av mina smartaste beslut som doktorand. Tack för att du blev kompis med stopped-flow-apparaten! Kombinationen av filosof och naturvetare gör dig till en verklig tillgång både som kollega och som person!

Fredrik och Erik,– vi började samtidigt, men ni hann före. Det blev tomt utan er! **Weixiao** och **Madde** – ni slog mig på uppploppet. Tur att ni är i närheten fortfarande så man kan få veta allt man behöver om att disputera men som ingen annan berättar.

Pontus – tack för den lysande, ursäkta explosiva, introduktionen till doktorandlivet. **Maria N** – du följde upp bra fast liiite tråkigare färg på proteinet!

Mikael – tack för alla hårt åtskruvade flaskor och annat jobbigt som du har fixat. **Etienne** – thanks for getting the UCP project going and the French cakes.

Maria S – du är en sån person som man blir glad av! Från första Biokemi 2 och framåt har du varit en riktig vän! Resten av NMR:arna – jag gillade att ha er i samma lab. **Anders** - du är den bäste man kan ha på labbänken mitt emot och **Linnéa** var ett fint tillskott!

Av de som hunnit några snäpp längre i karriären men som inte glömt hur man använder en pipett lär man sig mest - **Kristina, Rosie, Gergerly, Karin L. Rob** – tänker på dig varenda gång jag scannar en SDS-PAGE för du lärde mig hur man fixar till det utan bubblor. **Urszula** – tack för hjälpen med AQP2, timern behövde nytt batteri men mår annars bra.

Tack till mina examinatorer: **Martin och Jan**. Att diskutera Voet&Voet var överraskande trevligt!

Den här avhandlingen eller forskningen bakom hade inte kommit till utan en massa utrustning och datorer. **Lars och Bruno** – utan er hade det inte blivit något jobb gjort.

Det är riktigt kul att se gamla studenter bli nya doktorander - **Jennie, Rhawnie, Karin R och Petra** - jag minns var jag såg er först! Jag har alltid gillat undervisning, det var kul att hålla kurs med er: **Linda, Ida och David**. Och tack till **Örjan** för att ha hållit i trådarna!

Annette – vi har fortfarande inte haft något cykelrace Nymånegatan – Lundberglabbet! **Elin** – lycka till med kassörandet i Beer Club!

The new (or maybe not all so new anymore) members of the **Neutze&Westenhoff groups** – good luck with your work. **Cecilia** – tack för bra svar på alla möjliga slumpmässiga frågor jag kastar ur mig, inte minst nu på slutet.

All **new and former colleagues** at the Lundberg Laboratory – it was great to get to know you and good luck in the future!

Vägen till PhD gick via Chalmers. Nu minns jag inget längre av tentan i Transportprocesser utan bara mina fina vänner från **Bt02**. Vi måste träffas snart och titta på alla bebisar! Särskilt tack till **Helene** för att ha delat doktorandlivets upp- och nedgångar. Same, same but different.

Världen är bättre när man har en bror och syster. **Martin**, visa dem nu i Boston hur man gör när man springer! **Maria** – jag ser fram emot den dag då Dr. Frick och Dr. Alfredsson kan ha intelligenta konversationer under familjemiddagarna. Fast vi kan ju prata strunt också.

Mamma och Pappa – inget kan mäta sig med bra föräldar. Tack för att Solberga fortfarande är det tryggaste stället i världen att vara.

Erik och Astrid – tack för att ni stått ut med den senaste tidens undantagstillstånd. Nu är det färdigt, nu finns det tid att vara med er som betyder mest. Utan er är inget värt någonting!